Upscaling Estimation of Tropical Rain Forest Biomass/Carbon Stock Using TLS and Landsat-8 ETM+ Data

(*A case study from Royal Belum, Malaysia*)

SEMERE TESFAI

February, 2015

SUPERVISORS:

Dr. Y.A. Hussin

Dr. M.J.C. Weir

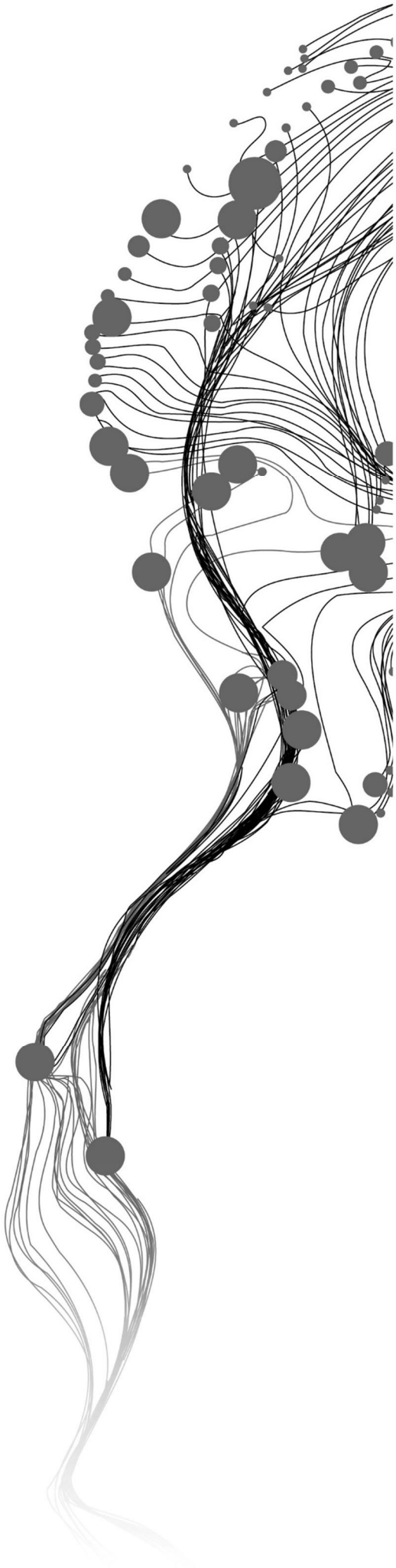

Upscaling Estimation of Tropical Rain Forest Biomass/Carbon Stock Using TLS and Landsat-8 ETM+ Data

(*A case study from Royal Belum, Malaysia*)

SEMERE TESFAI ABRAHAM
Enschede, The Netherlands, February, 2015

Thesis submitted to the Faculty of Geo-Information Science and Earth Observation of the University of Twente in partial fulfilment of the requirements for the degree of Master in Geo-information Science and Earth Observation.
Specialization: Natural Resources Management

SUPERVISORS:
Dr. Y.A. Hussin

Dr. M.J.C. Weir

THESIS ASSESSMENT BOARD:
Dr. Ir. C.A.J.M. (Kees) de Bie (Chair)

Dr. T. Kauranne (External Examiner, Arbonaut Oy Ltd. And Department of Mathematics and Physics – Lappeenranta University of Technology, Finland)

ABSTRACT

Forests sequester and store carbon stock and play an important role in the global carbon cycle through reduction of increasing carbon dioxide which leads to global warming. Estimation of the forest biomass/carbon stock using forest cover assessment over time is important to determine the extent of C emissions. In continuation to the relentless efforts to combat global warming and curb global risks associated, developing a method is increasingly important for monitoring, reporting and verification (MRV) mechanism of REDD+. A method to estimate aboveground biomass with sufficient accuracy to establish the increments or decrements of C stored in forests is needed. Thus, this study aims to develop a method which uses Terrestrial Laser Scanner (TLS) and Landsat-8 ETM+ data to upscale estimation of tropical rain forest above ground biomass/carbon stock.

FCD mapper and model was used to classify Landsat-8 ETM+ data of the study area. The FCD mapper classification generated 11 classes (one non-forest and 10 forest canopy density classes) with intervals of 10 percent. The accuracy of the classification was verified using ground truth and resulted in a strong correlation coefficient value of 0.84. In addition to this, the FCD mapper provides the area allocated to the different forest density classes. Out of 3,442 Ha of land classified, 34.5% is covered by water and the remaining is 65.5% covered by forest. The percentage share of each class out of the total area allotted for forest showed that, 95% of the area falls in the last 7 canopy density classes (class 4 up to class 10) of the FCD map.

Terrestrial laser scanner (TLS) was used to generate point cloud data from multiple scans (one in the center and 3 outer). The multiple scans were registered with an average standard deviation of 1.03 cm. From the registered scans, out of 698 trees 604 trees were extracted. This showed 87% tree detection rate using multiple scans (four scans). For each of the 604 trees, DBH and height was determined.

After the TLS derived tree parameters were obtained the relationship between basal area and FCD classes was examined and resulted in a strong correlation coefficient value 0.80. Then the relationship between FCD classes and biomass, calculated using allometric equation, was examined. Similarly, this resulted with a strong correlation coefficient value of 0.91. A model was then developed and validated with biomass prediction of R^2 0.73. The prediction model estimated the above ground biomass is 344 $MgHa^{-1}$ with RMSE 31%. The findings of the study are within IPCC (2006) mentioned 120-680 $MgHa^{-1}$ range of biomass. Similarly, Boscolo et al. (2001) study made in Malaysia which demonstrated an average above ground biomass of 428 tons/ha.

The main objective of the study was to develop a method which can be used for monitoring, reporting and verification (MRV) mechanism of REDD+. This method is considered to be operational, inexpensive, practical, rapid, and accurate. In the same time it can be applied frequently for monitoring forests on a larger scale base. This method can meet requirements mentioned above for REDD+ demands.

ACKNOWLEDGEMENTS

I am sincerely grateful to Joint Japan World Bank Graduate scholarship programme (JJ/WBGS) who granted me the scholarship to study in the esteemed University of Twente, Faculty of Geo-information Science and Earth Observation (ITC).

My deepest gratitude to Dr Yousif Ali Hussin, my first supervisor for his continuous guidance, invaluable positive suggestions, technical support and encouragement. His encouraging and respectful behaviour is unforgettable. I learnt more theoretical and practical skills from his great willingness to share his knowledge and experience.

I am deeply in debt and honoured to be among the last students of Dr Michael.J.C.Weir, my second supervisor for his supreme constructive and critical comments; and needless to mention also his sense of humour from the very start till the compilation of my study.

I would like to extend my sincere gratitude to Dr.ir.C.A.J.M. (Kees) de Bie, for his critical constructive invaluable comments during proposal and mid-term defence that backed me to shape my research.

I would like to thank the head of the Department of Natural resources drs. R.G. Nijmeijer (Raymond), the office of the Student Affairs and the Travel agency of ITC who stood and support me during those hard times.

I would like to acknowledge and express my thanks and appreciations for The University Technology Malaysia, Razak School of Engineering and Advanced Technology for their help and support to this research work. I am grateful for the support provided by UTM in housing, technical and instrumental support, transportation and data collection. I am in debt to all team members who join the fieldwork in Royal Belum, Perak, Malaysia. Special thanks and appreciations to Dr. Khamarrul Azhari Razak for the excellent management and organization of the fieldwork campaign and the Royal Belum Scientific Expedition. Dr. Razak and UTM are highly appreciated for their generosity in every aspect of the fieldwork campaign. The thanks and appreciations are extended to all team members of the Royal Belum Expedition, especially to Dr. Kian Pang Tan of UTM Johor Bahru, Malaysia.

Special thanks go to Anahita khosravipour, Phd. candidate of ITC, for her valuable theoretical and practical skills; and her guidance which helped me in my research work.

My deepest appreciation to all my fellow NRM and GEM students for the pleasant time we had and the work experience we shared from the different corners of the world. This has left irrevocable place in my heart and reminiscent sweet memories in mind.

Last but not least, I would like to thank all my friends here and abroad for their continuous support and comfort they provide me to feel right at home.

Semere Tesfai Abraham
Enschede, the Netherlands
February, 2015

Dedicated to Almighty God, the source of my inspiration, wisdom, excellence and integrity.

TABLE OF CONTENTS

LIST OF FIGURES

LIST OF TABLES

LIST OF EQUATIONS

LIST OF APPENDICES

LIST OF ACRONMYS

AGB	Above Ground Biomass
AVHRR	Advanced Very High Resolution Radiometer
COP	Conference of Parties
DBH	Diameter at Breast height
FAO	Food and Agriculture Organization
FCD	Forest Canopy Density
GPS	Global Positioning System
IPCC	International Panel of Climate Change
ITTO	International Timber Trade Organization
LIDAR	Light Detection and Ranging
MODIS	Moderate resolution Imaging Spectroradiometer
NOAA	National Oceanic and Atmospheric Administration
R^2	Coefficient of determination
RMSE	Root Mean Square Error
Radar	Radio detection and Ranging
REDD+	Reducing Emissions from Deforestation and Forest Degradation
SAR	Synthetic Aperture Radar
UNFCCC	United Nations Framework Convention on Climate Change
VHR	Very High Resolution

1. INTRODUCTION

1.1. Background

Climate change arises from greenhouse gas emissions (GHGs). The growing concentration of GHGs in the atmosphere trap the thermal radiation released from earth surface and increases temperature of the earth, which leads to global warming and climate change. Carbon dioxide (CO_2) is one of the principal gases that are contributors to the greenhouse effect in the atmosphere. It has been estimated that CO_2 increased from 1960 value of about 280 ppm to 379 ppm in 2005, which contribute to the increase of temperature by 1 ^{0}C to 4 ^{0}C (IPCC, 2007). Forests sequester carbon through the process of photosynthesis, when these forests are cleared or degraded the stored carbon is released to the atmosphere as CO_2 (Gibbs et al., 2007). Emission of CO_2 could be induced through natural process such as volcanic eruptions but is mostly caused by human activities. As a result our plant annually lose 7.3 million hectare of forest land and this contribute to 12% of global CO_2 emission (van der Werf et al., 2009). The reasons for the increase in greenhouse gases in tropical countries are deforestation, fossil fuel combustion and forest degradation (Gibbs et al., 2007).

Forest covers 31% out of the Earth's land surface and contains 283 Gts of carbon in biomass, 38 Gts of which is found in the soil (top 30 cm Litter) which exceed the amount of carbon (C) in the atmosphere (IPCC, 2007). Forests play important role in the global C cycle through reduction of increasing carbon dioxide (Brown, 1997). In particular, they provide a wide range of ecosystem services which are vital in supporting life (FAO, 2012). In light of this, retaining the existing forests and establishment of new forest is a cost effective option to mitigate global climate change (Zhang & Xu, 2003). Due to the above mentioned facts, estimation of the biomass/carbon pool of forests using forest cover assessment over time is important to determine the extent of C emissions.

According to Varjo & Mery (2001) forest cover changes can be done either by detecting actual forest and land use change or by executing an inventory twice on the same area (IPCC, 2007). Biomass is considered as a useful indicator of structural and functional attributes of forest ecosystems across a wide range of environmental conditions (Brown et al., 1999). Besides, biomass governs the potential carbon emission that could be released to the atmosphere (Lu, 2006). Being able to estimate biomass is therefore important to assess the role of forests in the global C cycle, particularly when defining its contribution toward sequestering carbon (Brown, 2002; Parresol, 1999). Measuring carbon in forests is important to the two key policies; the United Nations Framework Convention on Climate Change (UNFCCC) and the Kyoto Protocol (UNFCCC, 2014).

The UNFCCC adopted the Kyoto Protocol in Kyoto, Japan, on 11 December 1997 and it entered into force on 16 February 2005. It sets a collective global target of reducing GHG emissions by about 5% of 1990 levels by the first commitment period from 2008 to 2012. An amendment made to the protocol in Doha, Qatar, on 8 December 2012, known as the "Doha Amendment to the Kyoto Protocol", aims to reduce GHG emissions by at least 18 % below 1990 levels from 2013 to 2020 during the second commitment period (UNFCCC, 2014). This practice is expected to reduce the emissions to a safe level. The UNFCCC meeting in Conferences of parties (COP 15) introduced "REDD+" mechanism, which is concerned with both reducing and enhancing carbon stocks through actions that address deforestation, forest degradation, forest conservation and sustainable forest management (Cerbu et al., 2011). The UN-REDD is a collaborative programme that supports reduction of forest emission from degradation and deforestation in developing countries. Moreover, it supports in providing tools and monitoring methods to accurately estimate above ground carbon stock by reporting on stock changes. The design of a forest monitoring system includes measurement, reporting, and verification (MRV) according to internationally agreed requirements (UN-REDD, 2009).

Above ground biomass (AGB) is the total living biomass above the soil surface. Carbon forms approximately 50% of the AGB (Drake et al., 2002). For estimating above ground carbon stock either destructive or non-destructive methods can be applied. Although destructive measurement gives accurate result, it cannot be applied to large areas. Conversely, non-destructive method can be applied to large areas. Non-destructive method include approaches such as process based models, remote sensing based models, forest yield models, carbon flux measurement and forest inventory based approach (Qureshi et al., 2012).

Remote sensing (RS) is widely used for inventory. RS has increasingly attracted scientific interest because of precision of systematic and consistent data collection, a synoptic view, a digital format allowing fast processing of large data and covers vast areas, low in cost per unit area and the presence of correlations between spectral bands and vegetation parameters (DeFries et al., 2007; Lu, 2006; Patenaude et al., 2005). It also provides historical archives of span several decades and can therefore be used to reconstruct current and future time series. Remote sensing does not take direct measurement of AGB, it is supported by ground observations which are key to effective forest monitoring (DeFries et al., 2007).

Several studies had been done on estimation of biomass using remote sensing techniques and some could be mentioned among the proliferated papers presented. A study combined remote sensing imagery with LiDAR data (Lopez Bautista, 2012). Similarly, Lu et al. (2012) coupled Landsat and LiDAR data for above ground biomass estimation. This indicated the need for a tool or set of tools that will assist in providing information on forest condition for planning and monitoring. Over the past years, Forest Canopy Density (FCD), a biophysical model which uses forest canopy density to monitor forest canopy conditions over time. The model played a great role for sustainable forest management (Hussin, 2000). Likewise, terrestrial laser scanner (TLS) is gaining rapid interest as an efficient tool for fast and reliable three dimensional (3D) point cloud data acquisition in forest inventory (Maas et al., 2008). As such forest canopy density (FCD) mapper and terrestrial laser scanner (TLS) data could be used for estimation of above ground biomass/carbon stock.

1.2. Above Ground Biomass Estimation

Estimation of above ground biomass stock is based on features of vegetation such as canopy. It is necessary in estimating carbon stocks. Canopy extends from top to bottom in a three dimensional arrangement of canopy elements (leaves, branch and trunk of a tree) (Drake et al., 2003). Features like canopy height, diameter at breast height (DBH), basal area & steam diameter can be obtained from field and remote sensing data (Drake et al., 2003; Chave et al., 2005). Apart from remote sensing and field inventory, AGB can also be estimated using allometric equations, biophysical models, carbon flux models etc.

1.2.1 Remote Sensing Techniques for above ground biomass estimation

Remote sensing data provide a useful means for estimating biomass of forests. Most remote sensing studies describe the empirical correlation between forest biomass and the intensity of electromagnetic energy that is received by the instrument (Drake et al., 2002). The relationship with AGB can be direct, using remotely sensed data with different approaches, such as multiple regression analysis (Nelson et al., 2000; Zheng et al., 2004). AGB can be also estimated indirectly using remote sensors data of canopy parameters, such as crown diameter using multiple regression analysis or different canopy reflectance models (Phua & Saito, 2003; Popescu et al., 2003).

These relationships enable AGB to be used as an indicator for accurate forest covers change estimation (Hougton, 1996). By far made remote sensing is a potentially useful tool for spatial changes in forest condition (Harrell et.al., 1997; Lu, 2006). With the advantage that "Satellite based remote sensing systems observe the Earth at wavelengths ranging from visible to microwave, at spatial resolutions ranging from

sub-metre to kilometres and temporal frequencies ranging from 30 minutes to weeks or months" (Rosenqvista et al., 2003). Having various remote sensors with different spatial, spectral and temporal characteristics has made estimation of biomass promising and thus it is important to distinguish the type of sensors for the intended application of biomass estimation.

Remote sensors can be classified in to two types on the basis of the source of energy they use to collect information. Optical sensors regarded as passive sensors depend on sun radiation as their source of energy. While, active remote sensors like radar and LiDAR use their own energy (ITC, 2012). Optical remote sensing captures solar energy reflected from the earth's surface in the visible, near and middle infrared portion of the electromagnetic spectrum (~0.4 to 2.5 micrometer). They record spectral information for each pixel and allow the classification of the pixels into land cover classes (Patenaude et al., 2005).

On the basis of spatial resolution, optical sensor data can be classified as coarse, medium and high. Coarse resolution is used for global, continental and national scale biomass mapping such as NOAA AVHRR (Dong et al., 2003; Asner, 2001). Moderate resolution Imaging Spectroradiometer (MODIS) (Baccini et al., 2004), have been useful due to the good balance between spatial resolution, image coverage and frequency in data acquisition (Lu, 2006). Medium spatial-resolution ranges from 10 to 100 m. The most frequently used medium spatial-resolution data is Landsat data, which have become the primary source in many applications, including AGB estimation at local and regional scales (Lu, 2007; Phua & Saito, 2003; Sussman et al., 2006; Zheng et al., 2004). In monitoring land cover and land cover change at regional scales Landsat data being able to identify and map landscape features and patterns with sufficient detail and consistent data (Pax-Lenney et al., 2001). Besides, having proper spectral and spatial resolutions and relatively long historical datasets, as well as world-wide data availability which is free made it to be extensively applied for forest biomass or carbon estimation (Lu et al., 2012). Whereas very high resolution (VHR) data for small area biomass estimation such as IKONOS and QuickBird with 1 to 4 m resolution from aerial photographs or satellite images (Petrokofsky et al., 2012).

Optical sensor data has been widely used for estimation of AGB. Mostly, VHR data is used for AGB estimation. The data from satellite or airborne imagery requires image processing and interpretation such as, tree crown delineation, species identification and crown density to retrieve information (Katoh et al., 2008). Estimation of AGB done indirectly from the images and wall to wall (pixels) should be related with ground data. However, using VHR data tend to underestimate carbon in tropical areas due to dense canopy closure (Gibbs et al., 2007). There is also limit in the availability of good data to varying extent, since optical sensors relay on actual reflectance from the surface which can be obstructed due to the presence of clouds, aerosols and haze. In this kind of situations active remote sensors are more proper.

Radar also called as synthetic aperture radar (SAR) is an active remote sensor operating in microwave part of the electromagnetic spectrum (~ between 1 cm and 10 m for VHF5). SAR sends out a signal detect and record the wave properties of the returned echoes (the backscatter amplitude). The returned echo and the orientation of the electromagnetic wave (the polarization) are measured (Patenaude et al., 2005). The frequency transmit/receive configuration of radar data is stated by a three-letter code, the first letter designates the band of the radar and the last two letters state the polarization (horizontal/vertical) configuration. The different bands are C, L, K, S & X bands, that operate with different wave length and frequency provide different information about forest canopy (Gibbs et al., 2007). Whereas, polarizations have four combinations namely HH, HV, VH and VV (Lillesand et al., 2004).

Radar systems offer advantages for forest monitoring by operating day and night. In addition, radar signal cannot be impeded by moderate rain fall, penetrate cloud and ground cover. However, error increases in mountainous or hilly condition and response to estimation of biomass provides low results in forests with sparse large trees and heterogeneous forest structure (Gibbs et al., 2007; Patenaude et al., 2005).

LiDAR (Light Detection and Ranging) is an active remote sensor uses a pulse of laser energy with a wavelength (900 - 1064 nanometers) to travel from the sensor to the target (Drake et al., 2002; Lefsky et al., 1999). LiDAR sensors provide accurate measurements due to direct distance measurement. The distance measurement is calculated from the elapsed time from it is emitted by the sensor till it is received by. These measurements used to derive a precise three-dimensional characterization of an object, including forest canopy elements (Popescu, 2007).

On the basis of width of the beam and type of information collected from this return signal, LiDAR sensors are distinguished in to two broad categories (Figure 1). According to the former characteristics, as small footprints sensors with laser beam less than 50 cm and large foot prints with diameter greater than 5 m (Dubayah & Drake, 2000).

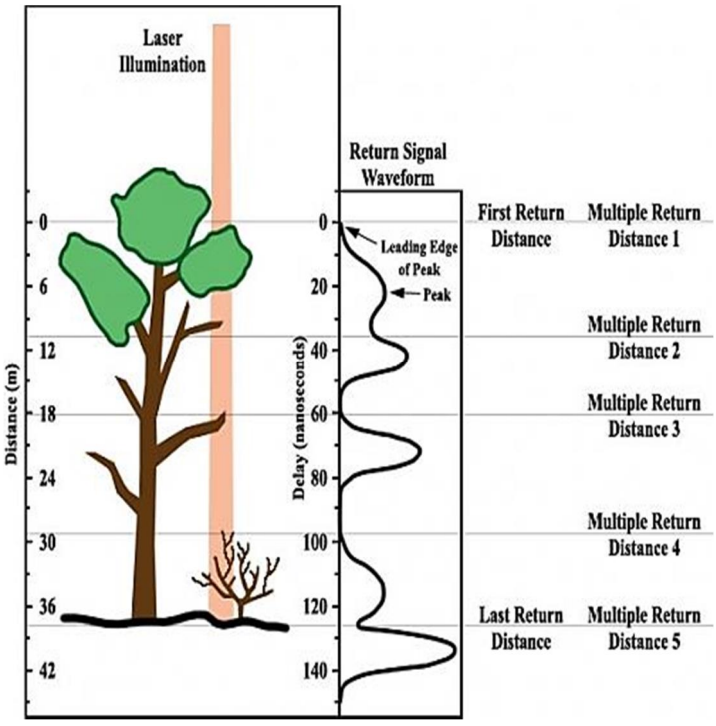

Figure 1. Illustrations of conceptual difference between waveform recording and discrete-return LiDAR devices (Lefsky et al., 2002)

Owing to the return from signal characteristics, sensors can be distinguished as discrete-return sensors. That measures the distance between the sensors and a target based on the elapsed time between the emission and return of the laser pulse. Waveform-recording scanning sensors, recording the shape and intensity of the pulse reflected from targets (Lefsky et al., 2002).

Laser scanners may be mounted on different platforms on satellites as space borne LiDAR system, on air craft as air borne LiDAR system, on tripod as terrestrial LiDAR system (Heritage & Large, 2009). The most common used formations of LiDAR systems are (1) airborne discrete-return scanning LiDAR, (2) airborne discrete-return profiling LiDAR, (3) airborne small-footprint waveform and (4) terrestrial LiDAR scanner. In this study, only terrestrial scanning will be investigated.

LiDAR is becoming very promising in monitoring forest cover with the advantage it offers accurate 3D forest structural characteristics which can quantify such as canopy heights, stand volume, basal area, and above-ground biomass (Dubayah & Drake, 2000; Lefsky et al., 2002). Studies made at plot level forest stand characteristic using estimation of tree parameters automatically proven its relatively high accuracy (Holmgren et al., 2003). Moreover, LiDAR has proved to be an efficient tool in the study of forest structure in a variety of forest environments (Drake et al., 2002; Lefsky et al., 1999; Magnussen et al., 1999).

A series of remote data collection technologies are now available to provide 'wall-to-wall' observation of carbon stock proxies and estimation over large areas using uniform method in a short time (Qureshi et al., 2012). According to DeFries et al. (2007), Drake et al. (2002), Lu (2006) and Patenaude et al. (2005), there is a growing interest in assessing biomass quantities accurately using remote sensors. However, there are still challenges encountered in quantification of forest carbon stock.

Several studies combined remote sensing techniques to get better result (Lu, 2006). The integration of optical remotely sensed imagery and LIDAR data provides improved opportunities forest structure

attributes and changes (Wulder et al., 2007). Integration of airborne LiDAR and hyperspectral digital imagery demonstrated the potential of assessing AGB inventory with high accuracy for individual tress and tree components (Popescu, 2007).

1.2.2 Allometric Equations

Biomass can only be measure directly through destructive sampling. Instead of this destructive method, estimates are developed through allometric relationship between weight of harvested trees and measurable tree parameters. Allometric equation is then defined as an equation which uses quantitative relationship between independent measurable tree dimensions, including trunk diameter and height and add up individual mass of a tree to assess biomass to provide relatively accurate estimates (Kangas & Maltamo, 2006; Phillips et al., 2002). The equation follows allometric regression models in estimating AGB, which is an important step in biomass estimation. DBH and height are the important tree parameters for biomass estimation, where DBH is measured at 1.30 m aboveground (FAO, 2004). More than 300 species can be found in 1 Ha of tropical forest (Oliveira & Mori, 1999). Grouping all species together and using generalised allometric relationships are highly effective in the tropics (Brown, 2002; Chave et al., 2005). Besides, Chave et al. (2005) developed a generic allometric equation and used a biomass regression model from DBH, height and wood specific gravity resulted with a bias of 0.5-6.5%. Thus, allometric equations are used because they are easy and non-destructive.

1.2.3 Biophysical Models for biomass estimation

The essence of a model is to relate quantitative data relate by a remote sensing system to biophysical features on the earth surface (Lillesand et al., 2004). These models synthesize and model absorbance and reflectance of vegetation, water, soil and other features of land. There are several biophysical models and can be grouped in different types of biophysical models on the basis of the relationship of remote sensing systems to the biophysical features of the earth. Although there is a wide classification of these models into a set of groups, for the purpose of biomass estimation we preferred to mention two set of groups. The first one as light use efficiency models, which use remotely sensed net primary production (NPP) to estimate maximum carbon assimilation rates to adjust suboptimal climate conditions using a series of simple climate response algorithms (Turner et al., 2003). The second one can be mentioned as simple empirical models, which use empirically derived algorithms that combine remotely sensing systems to vegetation properties. One example of these models is Forest canopy density model (FCD model) (Rikimaru et al., 2002).

FCD mapping and monitoring model was developed by International Timber Trade Organization (ITTO) in 1997. FCD uses forest canopy conditions over time. Using these principles a software named as FCD mapper semi-expert was developed to analyze satellite imagery (Rikimaru et al., 1999; 2002). The FCD mapper uses forest canopy density essential parameter. It comprises biophysical modelling and analysis of four indices. FCD mapping expresses canopy density in percentages, going from 0 to 100% in class of 10% for each pixel. It can only use imagery acquired by sensors that can measure thermal energy in addition to electromagnetic energy (visible-NIR-MIR). Landsat's TM and ETM+ sensors have the capability to do this (Gelens et al., 2010). This has advantage over the conventional RS methods which are based on qualitative analysis of information derived from ground truth and there is no direct involvement of remote sensing expert (Rikimaru et al., 2002; Musa et al., 2003). FCD-mapper offers useful system to the forester to implement FCD mapping process (Figure 2).

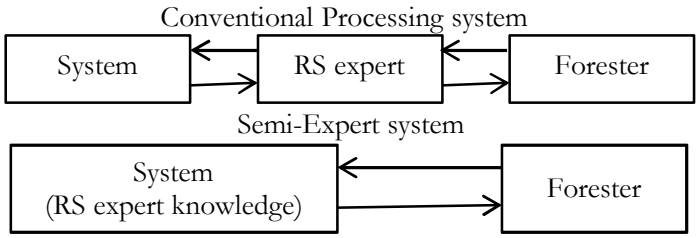

Figure 2. The concept of FCD-mapper (Rikimaru & Miyatake, 1997; Rikimaru et al., 2002)

Analysis of FCD mapping as compared to the convectional methodology is illustrated in Figure 3.

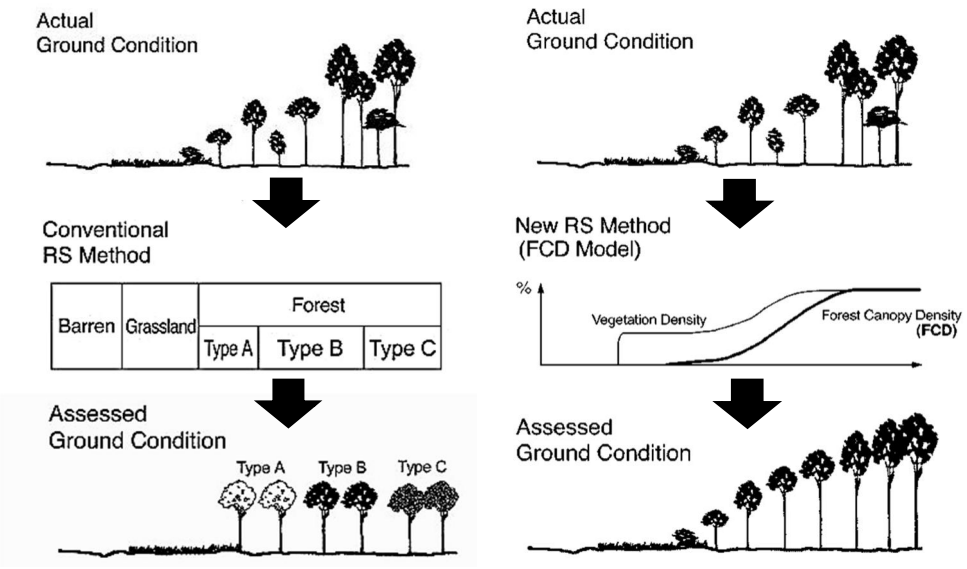

Figure 3. Analysis by FCD mapping model (Rikimaru et al., 2002)

1.3. Problem Statement

Climate change, a product of high carbon emissions have drawn global attention for high quality monitoring systems to estimate changes over time in biomass/carbon present on Earth's land surface (Petrokofsky et al., 2012). One of the main objectives of the study of the Earth's carbon cycle is measurement of biomass at different scales (global, regional and local) (Yao et al., 2011). Understanding the rate at which forest ecosystems change, grow, and add new biomass is important in developing more accurate estimates of factors contributing to GHG concentrations in the atmosphere and global carbon cycle (Hougton, 1996; Brown, 2002; IPCC, 2007). The general lack of accurate spatial forest biomass data has been considered as one of the most persistent uncertainties concerning global C budgets (Harrell et al., 1995).

Estimating change in forest cover uses biomass as an indicator of forest structural attributes. As part of the biomass, forest canopy refer to the proportion of the ground covered by the vertical projection of forest can be efficiently obtained from satellite images. It is a measure of the forest status (Gibbs et al., 2007). Since remote sensing images cannot measure forest biomass directly, both remote sensing and forest inventory data are required to estimate AGB (Drake et al., 2003; Rosenqvista et al., 2003).

Remote sensing images has been successfully assessing the distribution and rate of decline of tropical forests (Myers, 1980; Prince, 1987; Ringrose and Matheson, 1986; Ford and Casey, 1988; Iverson et al., 1989; Sussman et al., 1996). Various efforts using remote sensing have been performed to estimate carbon. Recent methods used airborne LiDAR data and very high resolution imagery. Although these methods managed to improve the accuracy to a significant extent, they are expensive, applicable only to small areas and the image interpretation is quite time-consuming and labour-intensive (Gibbs et al., 2007; Pax-Lenney et al., 2001).

Likewise metrics from synthetic aperture radar (SAR), such as backscatter, also tend to saturate in dense forest conditions (Drake et al., 2002; Gibbs et al., 2007, Kasischke et al., 1997; Patenaude et al., 2005) and have been shown to be insensitive to changes in AGB for secondary tropical forests with AGB levels greater than 60 Mg/ha (Luckman et al., 1997). In addition to this, a prior knowledge of the forest structural characteristics is required to analyse the SAR data adequately (Patenaude et al., 2005).

" The need to increase the accuracy and the spatial coverage of carbon accounting in forest ecosystems has both political and scientific rationales " (Patenaude et al., 2004). First, scientific rational is the issue of large uncertainty in estimation of carbon content. This urges to critically assess the accuracy and precision of the different remote sensing techniques and their applicability in geographically varied regions (Petrokofsky et al., 2012). Eventually to come up with cost efficient tools which provide accurate and rapid estimation (Patenaude et al., 2004). Second, political motive is countries ratifying the Kyoto protocol are required to report on emissions. Therefore, to discern and develop techniques for carbon inventory with sufficient accuracy to establish the increments or decrements of C stored in forests is progressively more important. The objective of UNFCCC is global in one hand but implementation is by individual nation on the other. To develop and run national-scale land carbon inventory systems will cost several million dollars per year. This would be the sum of national costs when we sum up the global cost nation-by-nation carbon (Bottom-up) inventory; this includes in turn the sum of individual project-scale inventories at national level. Therefore, the real total cost will be very high (Noble & Scholes, 2001).

One of the greatest challenges of REDD+ programmes is to develop methods that can measure forest biomass accurately and monitor the changes effectively at national level. Moreover, to standardize the wide differences between countries and assessment methods (Kankare et al., 2013). Eventually, REDD+ monitoring must be conducted in a manner that is reliable, transparent, and as accurate as possible, as well as feasible for developing countries and acceptable by the global community (Aikawa et al., 2012; Stolle et al., 2013).

Growing interest in the global C cycle demands estimating aboveground biomass with sufficient accuracy to establish the increments or decrements of C stored in forests is increasingly important (Henry et al., 2011). The current forest inventory estimation process is less accurate, has more bias from one to another person, expensive and time consuming. TLS can replace this inventory, as it is more efficient and accurate option for acquiring field data (Kankare et al., 2013). Presumably to alleviate the case with monitoring through provision of key constraint of data continuity, cost and technical capacity (DeFries et al., 2007). In line to this monitoring process, FCD Mapper which uses Landsat imagery data as the source data, a relatively inexpensive approach that requires only limited validation data. Moreover, FCD has been found to be technically simple, robust and quick, and can be applied frequently for forest monitoring on a large scale (Mon et al., 2012). To this the research aims to develop a method that combines FCD mapping and model with TLS data for upscaling carbon estimation. If successful the method can be used for estimation of carbon to meet the requirements of Kyoto Protocol and support the monitoring, reporting and verification (MRV) of REDD+ programme used for upscaling carbon estimation of forest AGB with low cost, less labour intensive, operational, practical and can be done frequently.

1.4. Overall Objective

The overall objective of this research is to develop a method to upscale the estimate of biomass/carbon in Royal Blum tropical rain forest in Malaysia using FCD Mapper, Landsat-8 ETM+ and Terrestrial Laser Scanner (TLS) data.

1.4.1 Specific objectives

1. To assess forest canopy density of tropical rain forest of Royal Belum using FCD Mapper and Landsat-8 ETM+ data.
2. To assess and validate FCD classes using field data (ground truth).
3. To investigate the relationship between FCD classes and biomass/carbon of tropical rain forest of Royal Belum based on TLS measurements.
4. Formulate a predictive model for up scaling biomass/carbon estimation using the above relationship.
5. To estimate, map and assess the accuracy of biomass/carbon stock in the study area.

1.5. Research questions

1. How is the application of classification of FCD mapper work with Landsat-8 ETM+?
2. What is the accuracy of FCD classification?
3. What is the relationship between FCD classes and biomass/carbon from TLS measurements?
4. How can a predictive model for up scaling biomass/carbon estimation using the above relationship be formulated?
5. What is the accuracy of the model for biomass/carbon estimation from TLS measurements?
6. How much carbon is stored in the study area?

Hypothesis

1. FCD can classify Landsat-8 ETM+ accurately (= 75%).
2. There is a significant (correlation) relationship between FCD classes and biomass/carbon (= 0.80).
3. Upscaling biomass/carbon estimation can be done (Predicted AGB is approximately equal to Observed AGB).

1.6. Theoretical Framework of Research

The research began with literature review followed by problem identification. After problem identification, research objectives and questions were formulated. Then, data required for research were defined and field work was carried out. Point cloud data, FCD classes and field data were analyzed. The results obtained were discussed and conclusions were drawn. The entire process is presented in Figure 4.

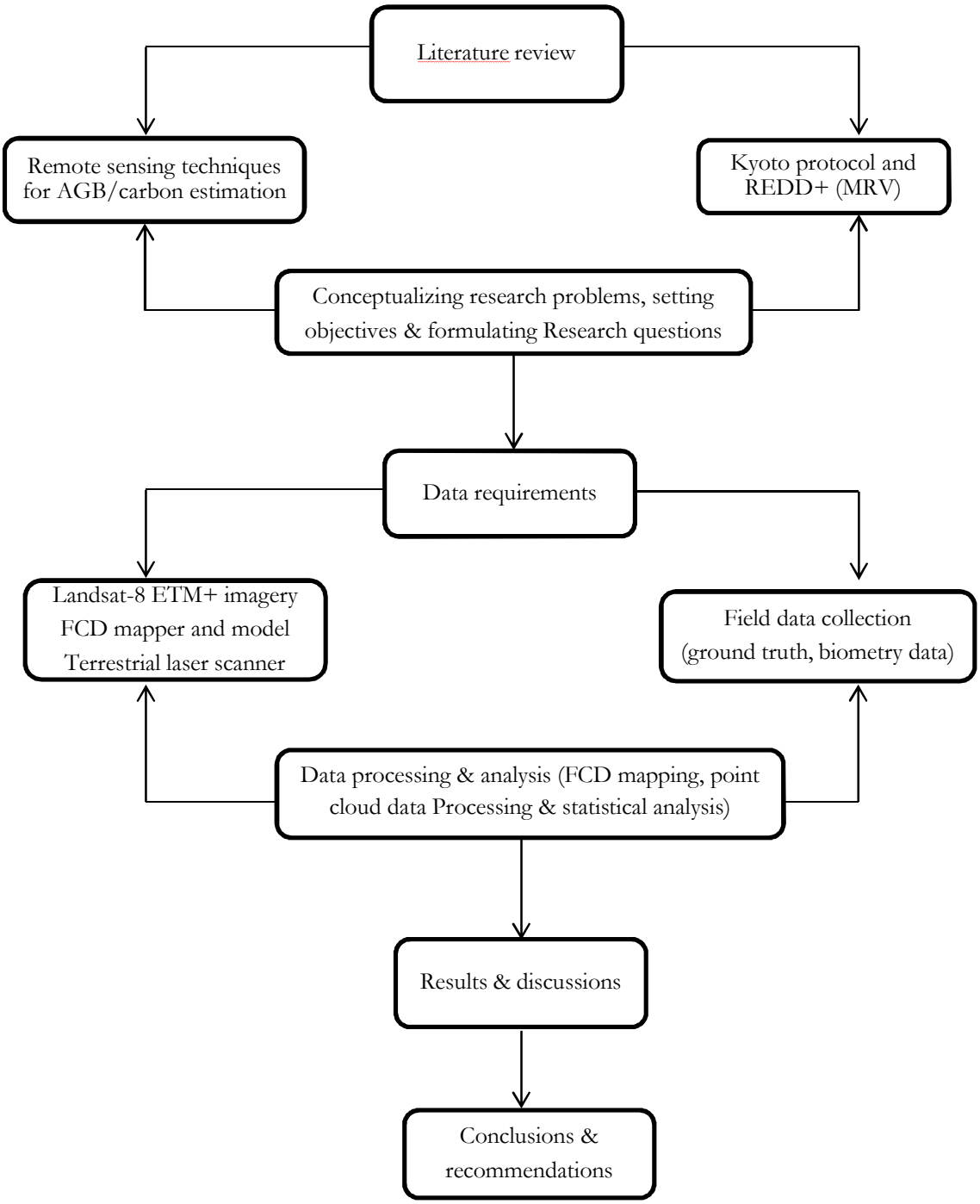

Figure 4. Theoretical framework of research

2. LITERATURE REVIEW, CONCEPTS AND DEFINITIONS

2.1. Literature Review

2.1.1 International agreements and reporting requirements

The two important international agreements related to measuring carbon in forests with concerns to the unrelenting issue of reducing GHGs emissions in the atmosphere are: the United Nations Framework Convention on Climate Change (UNFCCC) and the Kyoto Protocol (Patenaude et al., 2005).

2.1.1.1 Kyoto Protocol

Climate change is a response to addition of gases to the atmosphere, accumulation of GHGs beyond balance of atmosphere and biosphere pool exchange of gases would lead to detrimental effect on climate change. The situation steered international negotiations followed by agreements to reduce emission. This paved the road to Kyoto protocol related to UNFCCC with the goal to set international binding emission reduction targets to be achieved in first (2008-2012) and second (2013-2020) commitment periods. The emission reduction targets will enable stabilization of GHGs in the atmosphere naturally, reduce threats to food security and promote economic growth in a sustainable manner (Noble & Scholes, 2001).

Countries ratified the protocol are required to meet their targets through national measures. In order the countries to meet their targets the protocol presented other supplementary means by three ways of market-mechanisms: international emission trading, clean development mechanism and joint implementation. This is expected to encourage green investment by supporting parties to meet their emission targets in a cost-effective way. It is the first leap towards a truly global emission reduction regime which can provide the structural design for the future international agreement on climate change (UNFCCC, 2014).

Many tropical countries have at least one inventory of all or part of their forest area, although many of the inventories are more than 10 years old and very few have repeated inventories. Data from these inventories can be converted to biomass carbon in one of two ways depending upon the level of detail reported (Brown, 1997). The Kyoto Protocol forthcoming need to determine sources and sinks of carbon resulting from land-use change and desperately demand methods that can determine biomass accurately, repeatedly, and inexpensively. Provided that these methods are available, they would be used routinely by the world's nations (Houghton et al., 2001).

2.1.1.2 REDD+

Tropical countries comprise 50% of the species on the earth in less than 5% of the earth's land area. These forests sequester and store 375 billion metric tons of carbon and provide a wide range of ecosystem services to human beings. They depend directly or indirectly on the services that are provided by the forest. Forests are exploited to obtain these services in the form of timber, food and other goods, which directly or indirectly provide income. Over-exploitation, leading to deforestation and forest degradation has become the major contributors to emissions in tropics. As a remedy, payments to ecosystem service could reduce deforestation in forest dependent communities, the UNFCCC introduced the REDD+ in national conference of Bali Action Plan in the year 2007 and was launched in 2008 (Stolle et al., 2013).

The REDD+ programme has 56 member countries from Africa, Asia-pacific and Latin America. It focuses on direct support to design and implementation of national programmed and complementary support to different incentives, training, methodology, approaches and development of national systems for measuring, reporting and verification (MRV).

MRV activities include field work, data processing, analysis and reporting (UN-REDD, 2009). The three components of MRV are defined as:

- **Measuring:**- includes both actual and physical measurement of emissions or removal from forest area as well as the calculations used from simple formula to sophisticated models.
- **Reporting:-** related to the documentation of estimates of GHGs, the methodology used, quality, quantity and uncertainty.
- **Verification:-** involves internal and international checking of the inventory.

Under the UNFCCC, the REDD+ mechanism agreed at the COP-16 of the UNFCCC in 2010 implementation of mitigation action through: reducing from deforestation, forest degradation, conservation of forest carbon stocks, sustainable management of forest and enhancement of forest carbon stocks (Petrokofsky et al., 2012). Later at the COP 17 the REDD+ mechanism stated that implementation should be at national level or if possible at sub national level. Countries should include monitoring plans with institutional, legal and procedural arrangements for estimating emissions and mechanism for reporting and archiving. The mechanism supports countries to develop cost-effective, robust, operational and compatible monitoring systems. Moreover, the monitoring systems need to be coherent to UNFCCC regulations.

Monitoring is crucial to assess emission levels so that compensation could be earned from emission reductions. Changes in carbon stock can be estimated through land use yearly inventory, conversion of forest to other land use and stocks of carbon that are subjected to change or not. Since it is not possible to measure all emissions and removals, the estimations can be made for emission rate before and after change in land use using inventories with different levels of complexity called "tiers". Generally, there are three Tiers named as Tier 1, Tier 2 & Tier 3. Tier 1 uses globally available sources (deforestation rate, agriculture production statistics, fertilization rate etc.). Tier 2, uses emissions and stock change based on country or region-specific data whereas Tier 3 uses methods which include models and inventories tailored to address unique national circumstances. Inventories using higher tiers have improved accuracy and reduced uncertainty. In developing a monitoring system care should be taken to take in to account the scope, estimation methodology, cost and data needs. For estimation methodology REDD+ use remote sensing and thus active remote sensors radar and LiDAR are the most commonly used remote sensors. The spatial and temporal resolution of Landsat data provide source data for monitoring, with historical data archives of past and future (Stolle et al., 2013).

2.1.2 Terrestrial Laser Scanner

The principle of Terrestrial Laser Scanner (TLS), also known as ground based LiDAR, is based on a highly collimated laser beam that scans over a predefined solid angle in a regular scanning pattern and measures the time-of-travel of the laser signal. The scanning range of the midrange terrestrial system allows distance measurements between 2 m and 800 m (Kankare et al., 2013). TLS is composed of a laser range finding system and the beam deflection unit; the instrument is mounted on a tripod. TLS generates 3D (three dimensional) point clouds consisting of several million 3D points densely representing an object surface in a polar measurement mode by scanning in two directions and measuring distances (Figure 5). These points provide the possibility to document forest both vertically and horizontally in great detail. Terrestrial Laser Scanners are composed of rapid pulse lasers, precisely calibrated receivers, precision timing, high-speed micro controlled motors, precise mirrors and advanced computing capabilities (Fowler & Kadatskiy, 2010).

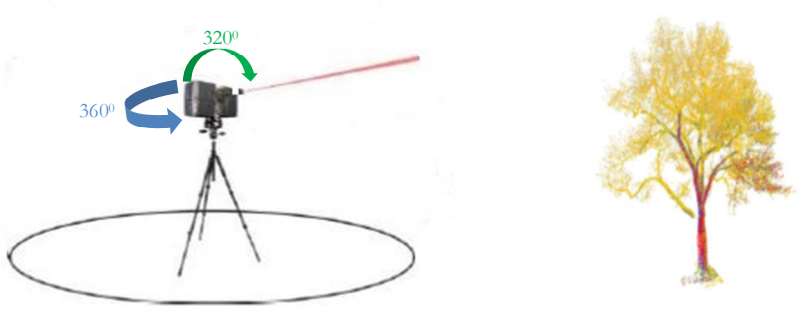

Figure 5. Illustrations of scanning mechanism of a TLS scanner (Dassot et al., 2011) and point cloud data of a tree

There are different TLS instruments currently on the market and these can be categorised according to the following criteria (Figure 6 and Table 1).

1. **Range measurement principle**:- Most scanners use measurement of the time-of-flight to determine range. The precision of measurement is usually limit to 5-10 mm. some scanners use phase modulation techniques to achieve a higher measurement precision of 1-3mm.
2. **Beam deflection principle**:- scanners scan an object surface with the beam mirrors sequentially in two scanning directions, deflected by galvanometric, polygon wheels, and rotating elliptical mirrors; rotation of the instrument or combinations.
3. **Field of view**:- Most laser scanners offer a panoramic 360^0 horizontal field of view with a vertical opening angle between 80^0 and 135^0, with the latter offering the possibility of hemispheric scans. Some scanners offer a camera-like rectangular field of view (Maas et al., 2008).

a. Riegl VZ-400 b. Riegl LMS-Z 420i c. Leica HDS6100

Figure 6. Example of the latest scanners (www.riegl.com; www.leica-geosystems.com)

Table 1. Specifications of the examples of terrestrial laser scanners shown in figure 6

Type	Riegl VZ-400	Riegl LMS-Z 420i	Leica HDS6100
Ranging method	Pulse ranging (full-waveform)	Pulse ranging	Phase shift
Wavelength (nm)	1,550 (near-infrared)	1,550 (near-infrared)	690
Max. Measurement range (m)	280 - 600	350 – 1,000	0.4 - 79
Accuracy (mm)	3	10	5
Beam divergence (mrad)	0.3	0.25	0.22
Footprint size at 100 m (mm)	30	25	22
V x H field of view	100^0 X 360^0	80^0 X 360^0	310^0 X 360^0
Acquisition rate (pts/s)	Up to 122,000	Up to 11,000	Up to 500,000
Weight (kg)	9.6	16	14
Operating temperature	0° to +40° C	0° to +40° C	-10° to +45° C

These scanners follow two scanning mechanism to capture measurements: single scanning or multiple scanning methods (Figure 7). Single scanning method as its name implies uses only one location of the scanner (e.g. center of the plot) and only one scan is made. This method allows fast and easy method of tree scanning, but occlusion is unavoidable. Occlusion refers to the hiding of far trunks, branches, and foliage by closer objects. In the multiple scan method, several scans (three to four) are made in and around the object and it is much more time consuming. This allows for increased field measurement, ensures the most complete 3D description of objects and information about the trees from more than one direction (Bienert et al., 2006; Dassot et al., 2011). Registration is done to integrate the multiple scans using one reference point (Côté et al., 2009).

.

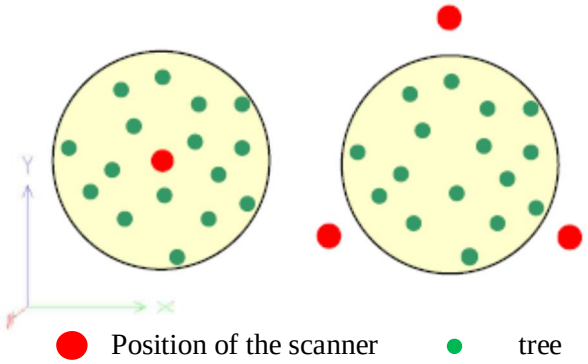

Figure 7. Single scan and multiple scan mode (Bienert et al., 2006)

2.1.2.1 Application of Terrestrial Laser Scanner (TLS) for Above Ground Biomass Estimation

Currently, AGB estimation is based on allometric relationships of DBH and heights and generally leads to errors. LiDAR is becoming a propitious technique in monitoring forest with the ability to provide detailed forest structure (Patenaude et al., 2005). TLS has the potential to provide more detailed information on canopy structure. The introduction of TLS measurement in forestry enables precise tree stand parameters measurement such as diameter at breast height (DBH), which is the crossection of trunk of the tree. Other such as canopy height, crown diameter, stem density (trees per unit area), basal area e.t.c. which are used to provide information about timber quality, volume, biomass and forest growth. The positional accuracy of TLS is within 0.5 -10 cm which is more than the accuracy of airborne LiDAR, 0.1 to 1 meter (Yang et al., 2013).

Dassot et al. (2011) mentioned the potential of TLS in the future to improve forest measurements by providing faster and more detailed information of the forest structure than the time-consuming manual techniques. Moreover, it provides information inaccessible to large-scale airborne LiDAR measurement. They also mentioned that studies were made on plot level forest inventory and to mention some: standard denderometric parameter (DBH, height, stem volume, basal area & wood volume), species identification from bark analysis, external trunk quality, forest canopy characterization and advanced modelling of tree structure etc. The results show resonable accuracy, with approximately +5 cm errors in defining tree location, +1.7 cm in detemining DBH. These accuracies are very hard to achieve using human hand measurements using different ground truth data collection tools e.g. diameter tape, calliper, Haga hypsometer, etc.

DBH is a critical forest inventory parameter in estimating biomass, timber volume and forest growth. Various studies indicated also the provision of TLS is more straightforward, which means for directly retrieving DBH values, usually by fitting circles, cylinders, or free-form curves to scattering points (Hopkinson et al., 2004, Pfeifer et al., 2004; Thies et al., 2004). Similarly Watt & Donoghue (2005) and Yao et al. (2011) in a study made on measurement of forest structure demonstrated a very strong linear relationship between DBH measured in the field and TLS data. Moreover, Bienert et al. (2006) application of TLS for determining forest inventory parameters using single and multiple scan got very good results namely: automatic detection of tress 97.4% using single scan in primary forest.

Furthermore, Antonarakis (2011), Kankare et al. (2013), Maan et al. (2014), Maas et al. (2008), Seidel et al. (2013) and Tansey et al. (2009) all report accuracies for tree detection of 52% in dense stocked plantations. These results showed that TLS could be used to measure tree DBH, height and stem volume accurately and estimated AGB and carbon for individual tree or at a plot level.

The frequent scan records of these measurements allow to develop forest inventory for temporal monitoring of forest (Watt & Donoghue, 2005). This provides the tools and methods that are required to support the monitoring, reporting and verification (MRV) for REDD+ projects.

2.1.3 FCD Mapping and Model

2.1.3.1 Characteristics of the FCD mapping and model

The FCD mapper and model is composed of bio-physical phenomenon modelling and analysis of the data extracted from four indices: Advanced Vegetation Index (AVI), Bare Soil Index (BI), Shadow Index or Scaled Shadow Index (SI, SSI) and Thermal Index (TI) (Rikimaru et al., 2002). The indices have some characteristics as shown below in Table 2. It utilizes integrated data from the four indices. Fig. 8 illustrates the relationship between forest conditions and the four indices. Vegetation index is a response to all of vegetation items such as the forest, shrub land and the grassland. As the forest density increases so does the Shadow index increases. Similarly, as the vegetation quantity increases the Thermal index increases. Presumably black coloured soil area shows high temperature. Eventually, Bare soil index increases with degrees of ground. The model then calculates the four index values for every pixel are.

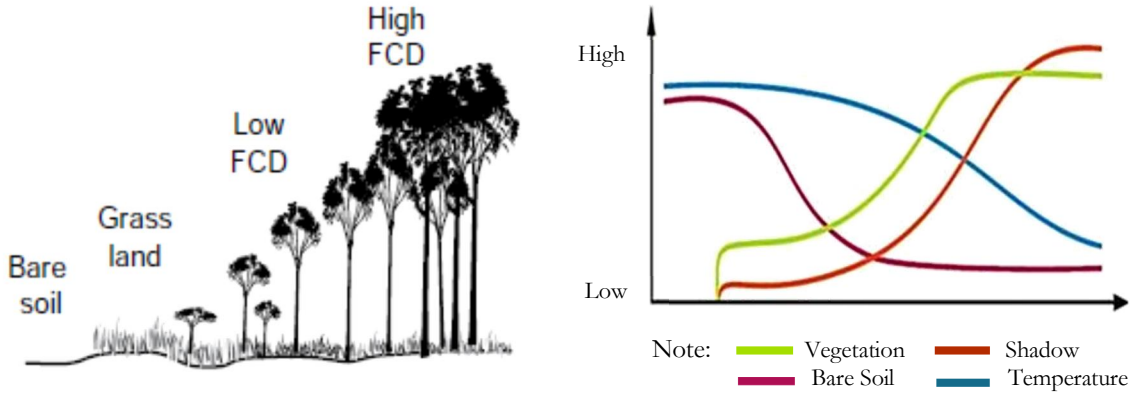

Figure 8. Illustration of the relationship between forest conditions and the four indices (Rikimaru et al, 2002; Chandrashekhar et al., 2005)

FCD value increases with increase in SI value; this is due to the presence of more shadow when there are more trees. On the other hand, TI decreases with decrease in BI. This means less bare soil and this indicate low TI value. The analysis shown in the above graph indicates that VI reaches maximum value earlier than SI. The combination characteristics between the four indices are presented in Table 2.

Table 2. Combination characteristics between four indices

	Hi- FCD	Low-FCD	Grass land	Bare Land
AVI	Hi	Mid	Hi	Low
BI	Low	Low	Low	Hi
SI	Hi	Mid	Low	Low
TI	Low	Mid	Mid	Hi

Source (Rikimaru & Miyatake, 1997) and (Rikimaru et al., 2002)

According to Rikimaru et al. (2002), the integration process of the four indices is presented in the following sections.

1. Advanced vegetation Index (AVI)

When assessing the vegetation status of forests, the FCD model first examines the characteristics of chlorophyll-a. The chlorophyll-a absorbs the red light and totally reflects the near-infrared light. This property is applied to compute the Advanced vegetation Index (AVI) using this formula:
B1-B7: TM Band 1-7
B43 = B4-B3 done once the data is normalized.
CASE-a B 43 < 0 AVI = 0
CASE-b B 43> 0 AVI = ((B4 +1) x (256-B3) x B 43) 1/3

2. Bare Soil Index (BI)

Estimating vegetation status in situations where there is low vegetation cover of the area (less than half), using vegetation index not reliable and thus bare soil index is incorporated by the model. The information of bare soil is extracted from the medium-infrared band of the satellite image. The logic behind then work on the inverse relationship (negative correlation) of the soil and vegetation status. The analysis combining these two indices will assist to assess the conditions of the forest in a sequence starting with more vegetation cover to a low vegetation cover left no more than bare soil.
BI= [(B5+B3)-(B4+B1)] / [(B5+B3) + (B4=B1)] x 100 + 100; 0 < BI <200

3. Shadow Index (SI)

Forest is a three dimensional in structure. Information on the forest structure can be extracted from combination of RS data of the forest and shadow of the forest by itself. Forest stands have various crown arrangements and this governs the shadow pattern. The pattern of the shadow influences the thermal information and this in turn affects the spectral responses. Thus, mature forest stands have more shadow index than young aged stands. The formula uses low radiance (visible bands) to compute shadow index.
$SI = ((256\text{-}B1) \text{ X } (256\text{-}B\ 2) \text{ X } (256\text{-}b3))^{1/3}$

4. Thermal Index (TI)

Inside the forest the temperature is relatively cool, the cooling process is associated with the canopy and the leaves. The forest canopy acts as a shield in blocking the sun energy in one way and enhancing the absorption in the other. The evaporation process from the leaf surface also protects warming, to add cooling effect to the forest. The thermal index is generated from these phenomenons. The thermal band of the TM data provides the thermal information. Temperature calibration for the thermal infrared band into the value of ground temperature has been done using the following equation:
L + L min + ((L max-L min)/255) x Q
Where:
L max: value of radiance = 1.500 mw/cm2/str (Q=0)
L min: value of radiance = 0.1238 mw/cm2/str (Q=255)

The FCD mapper and model produces 11 classes (one non-canopy and 10 canopy classes) with intervals of 10 percent. To verify the accuracy of the density maps, ground truthing need to be carried out to compare the crown density. The model is founded on the growth phenomenon of forests, this enables to monitor forest conditions transformation including degradation and progress of reforestation activities overtime (Rana & Vickers, 2005). Furthermore, Jamalabad & Abkar (2004) applied forest canopy density for monitoring using satellite images in Iran. The study showed a strong relationship between FCD classes and field observations.

Use of the FCD model upgrades the planning and management capacity of decision-making and increases information available to forest managers. The use of the semi-expert system in FCD Mapper is user-friendly and provide accurate and unbiased data on forest status in easy format to understand (Hussin, 2000; Rikimaru et al., 2002). In addition to this, a study made in estimating the FCD of mixed deciduous

forest in Myanmar and found that FCD mapper and model is cost-effective and saves time (Mon et al., 2012).

Previous research conducted in Australia and Korea suggested that FCD is a quick and robust method and has a promise for forest monitoring (Baynes, 2004; Kwon et al., 2012). Similarly, study made on implantation of FCD model to monitor deforestation in India has proven to be an effective means for measuring forest cover assessment in a very short period (Deka et al., 2012, and Chandrashekhar et al., 2005). In addition to this, Panta & Kim (2006), Kandel et al. (2004) and Deka et al. (2012) used FCD for the spatio-temporal assessment of the tropical forest of Nepal and India using Landsat imagery and found that pixel based forest canopy mapping consistently detected the dynamic change of the forest.

2.2. Concepts and definitions

2.2.1 Above Ground Biomass (AGB)

AGB is defined as "all biomass of living vegetation, both woody and herbaceous, above the soil including stems, branches, bark, foliage, bark and stumps"(IPCC, 2006b). According to Drake et al. (2002) AGB is the total amount of carbon within living tissues present above the soil surface in a specified area. Carbon forms approximately 47-50% of the AGB (Drake et al., 2002; IPCC, 2006a).

The potential carbon emission that could be released to the atmosphere depends on biomass. Changes in biomass have been associated the roles and impacts of biomass on carbon cycles (Lu, 2006). " Carbon inventory consist of estimation of stocks and fluxes of carbon from different land-use systems in a given area over a given period and under a given management system " (Ravindranath & Ostwald, 2008).

2.2.2 Pool, stock and flux

According to Noble and Scholes (2001) definitions a 'pool' is a reservoir of carbon such as terrestrial vegetation (above ground and below ground) or surface ocean waters. 'Stock' refers to the amount of carbon each pool contains and 'flux' refers to transfer of carbon between pools through different process including photosynthesis, respiration and combustion. The Kyoto Protocol refers to the flux between the terrestrial carbon pool and the atmosphere as 'emissions' and the opposite flux between the atmosphere and the terrestrial carbon pool as 'removals' (often referred to as 'uptakes' in other literature about the Protocol, or as a 'sink').

2.2.3 Forest Canopy Density

Forest canopy density refers to the proportion of the ground covered by the vertical projection of forest floor (Howard, 1991). According to Lefsky et al. (1999) it is the percentage or fraction of sky obscured by vegetation. This can be efficiently obtained from satellite images as a measure of the forest status (Sussman et al., 2006). To analyze the forest status satellite images were used and estimates of the crown density were created using Forest Canopy density (FCD) mapper and model.

2.2.4 Point Cloud Data

The outputs of the TLS were presented in a point cloud data. For each return the point cloud data records position and intensity (x, y, z, i) as well as RGB or colorized point cloud data from image acquired. These point cloud data was further processed from plot level to tree level parameters such as tree height and diameter at breast height (DBH).

2.2.5 Upscaling

Much effort has gone into developing tools and models that can 'scale up' or extrapolate destructive harvest data points to small scales based on proxies measured in the field or from remote sensing instruments (Brown, 1997; Chave et al., 2005). Previous studies come up with above ground woody carbon mapping with very high resolution digital camera imagery 0.45 m resolution (Maharjan, 2012) and Geo-eye imagery with and 0.5 m resolution map (Lopez Bautista, 2012). As a continuation to the underlined efforts, this study produced upscaled carbon map of the study area using Landsat-8 ETM+ (30 X 30 m resolution) data.

3. STUDY AREA, MATERIALS AND METHODS

3.1. Study area

3.1.1 Overview of the study area

The study area Royal Belum State Park (RBSP) lies in the northerly region of the State of Perak in northern Peninsular Malaysia (Figure 9). It is situated between 101^0 21'14.495" - 101^0 24'51.07" E and 5^0 33'47.966" - 5^0 36'39.625" N. One of the oldest tropical rainforests in the world (older than Amazon and the Congo) and remains one of the largest untouched forest reserves with amazing flora and fauna in Malaysia. RBSP is bordered by Thailand on the north, Temengor Forest Reserve to the south, the state of Kelantan to the east, Sungai Gadong in the west. The park is a protected area which encompasses a total area of 117,500 ha (Royal Belum State Park, 2003).

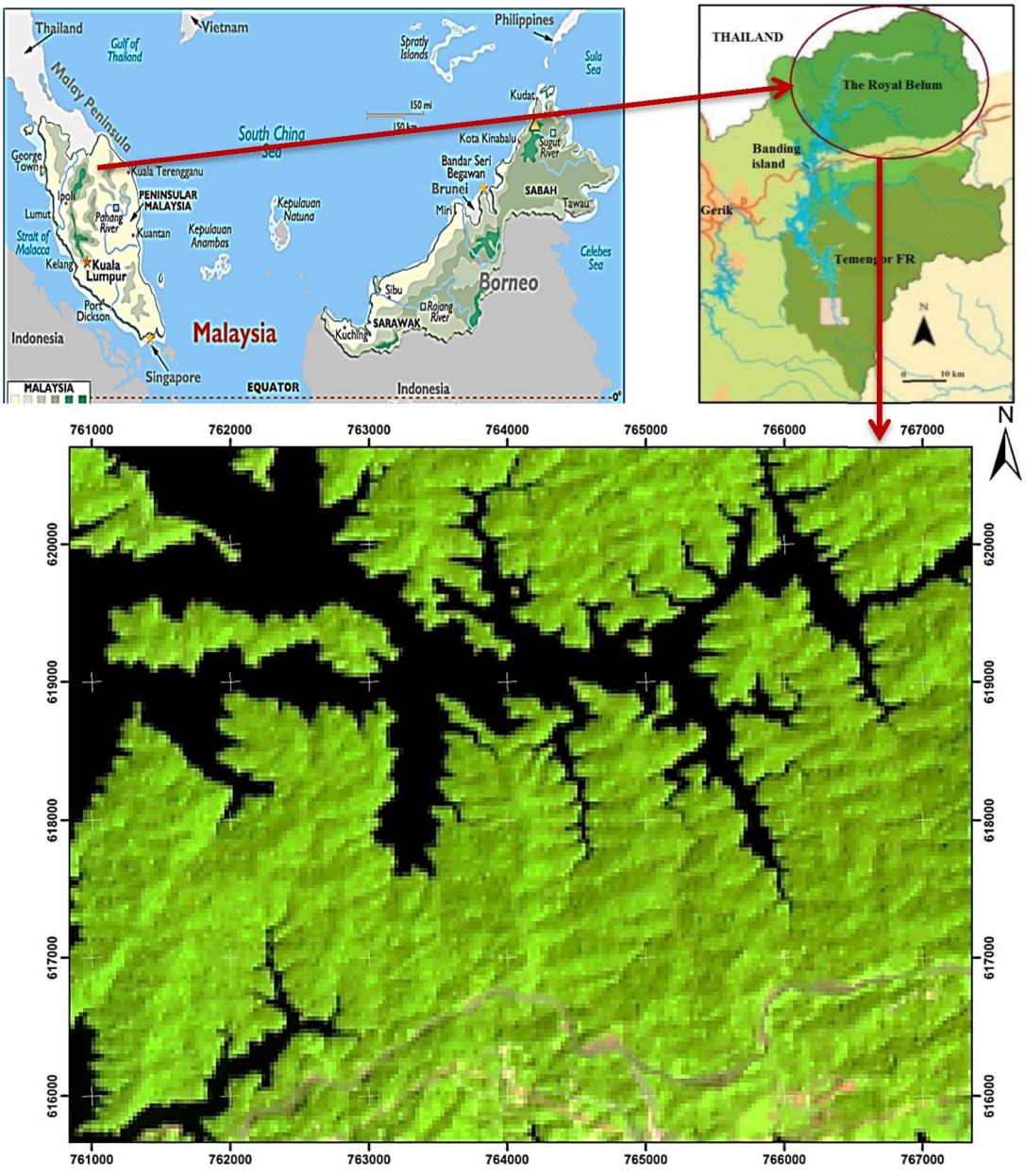

Figure 9. Location map of the study area

3.1.1.1 Topography

The landscape of RBSP consists of forest, small areas of grassland, and abandoned agricultural plots, as well as a large man-made lake, Tasik Temengor. It extends from 260 m asl (above sea level) to 1,533 m asl (Royal Belum State Park, 2003).

3.1.1.2 Climate

The area benefits a tropical climate with high temperatures and high humidity throughout the year. The average minimum temperature is 23 ^{0}C and maximum 32 ^{0}C.

3.1.1.3 Rainfall

The area receives an average annual rainfall 2,205 mm. The wettest months are May to October on the west coast, while on the east coast the wettest months are September to December.

3.1.1.4 Vegetation

The main forest cover types found are mainly lowland Dipterocarp, hill Dipterocarp and upper Dipterocarp forests. The forest is characterized by tropical rain forest species; mostly dominated by dipterocarp species.

3.2. Materials

3.2.1 Data set

Landsat-8 ETM+ imagery obtained on February 11, 2014 is used. During the field work, point cloud data was collected using Riegl VZ-400 Terrestrial Laser Scanner (TLS) point cloud data was collected during the field work.

3.2.2 Equipment's used

Table 3 is showing the list of instruments used during the field work.

Table 3. List of equipment's used in field work

S.N	Type of Equipment	Use
1.	iPAQ	Navigation
2.	Garmin eTrex vista GPS	Navigation
3.	Suunto compass	Directional measurement
4.	Suunto clinometer	Slope measurement
5.	Leica DISTO D5	Height measurement
6.	Hemispherical camera	Crown cover measurement
7.	Spherical densiometer	Crown cover measurement
8.	Diameter tape (5m)	DBH measurement
9.	Measuring tape (30m)	Distance measurement
10.	Data record sheet	Field data recording

3.2.3 Software used

1. FCD-mapper

FCD mapper was used generate canopy density classes from Landsat-8 ETM+ imagery. It uses four indices: AVI, BI, SI and TI and integration of four to generate one non-forest and 10 forest canopy density classes.

2. RiSCAN PRO V1.8.1

The software used for processing of point cloud data. To mention some of the task carried out include:

- Registration
- Filtering
- Cleaning
- Creating plane
- Creating polydata
- Visualization using different viewer modes (RBG, intensity, range & height).
- Tree extraction

3. CAN-EYE V6.3.13

CAN-EYE is open source software used to generate canopy density percentage of plots from hemispherical camera images, also known as fisheye or canopy photography collected from the field work. The software helps to classify the image in to sky and vegetation, and then it provides the plot canopy percentage.

4. Other software used

Furthermore, Landsat imagery was also processed by ERDAS imagine 2013 and ArcGIS 10.2. Statistical analysis was done using R studio, MATLAB, SPSS and Microsoft Excel. Other Microsoft office 2010 such as MS Word, MS Power Point was used for statistical analysis and thesis writing.

3.3. Methods

The method of this research consists of three major parts: satellite data processing, field data collection, terrestrial LiDAR processing and model development. Landsat-8 ETM+ imagery was processed using FCD mapper and FCD map with 11 classes was generated. Field work was done for ground truth and to collect DBH, height, crown diameter and plot level crown density. Furthermore, using TLS multiple scan of 32 plots were carried out to obtain point cloud data. The plot level point cloud data was processed to extract tree parameters such as DBH & height. The FCD classes were validated using field data. The relationship between FCD classes and TLS tree parameters was analyzed. A model was developed from tree parameters of acquired from TLS. This model was validated using field data. A regression model developed for upscaling biomass/carbon from tree parameters from TLS and validated FCD classes. Using map calculator carbon map was developed and amount of carbon of the study area was obtained. The process of the research methodology is presented in the flowchart in Figure 10.

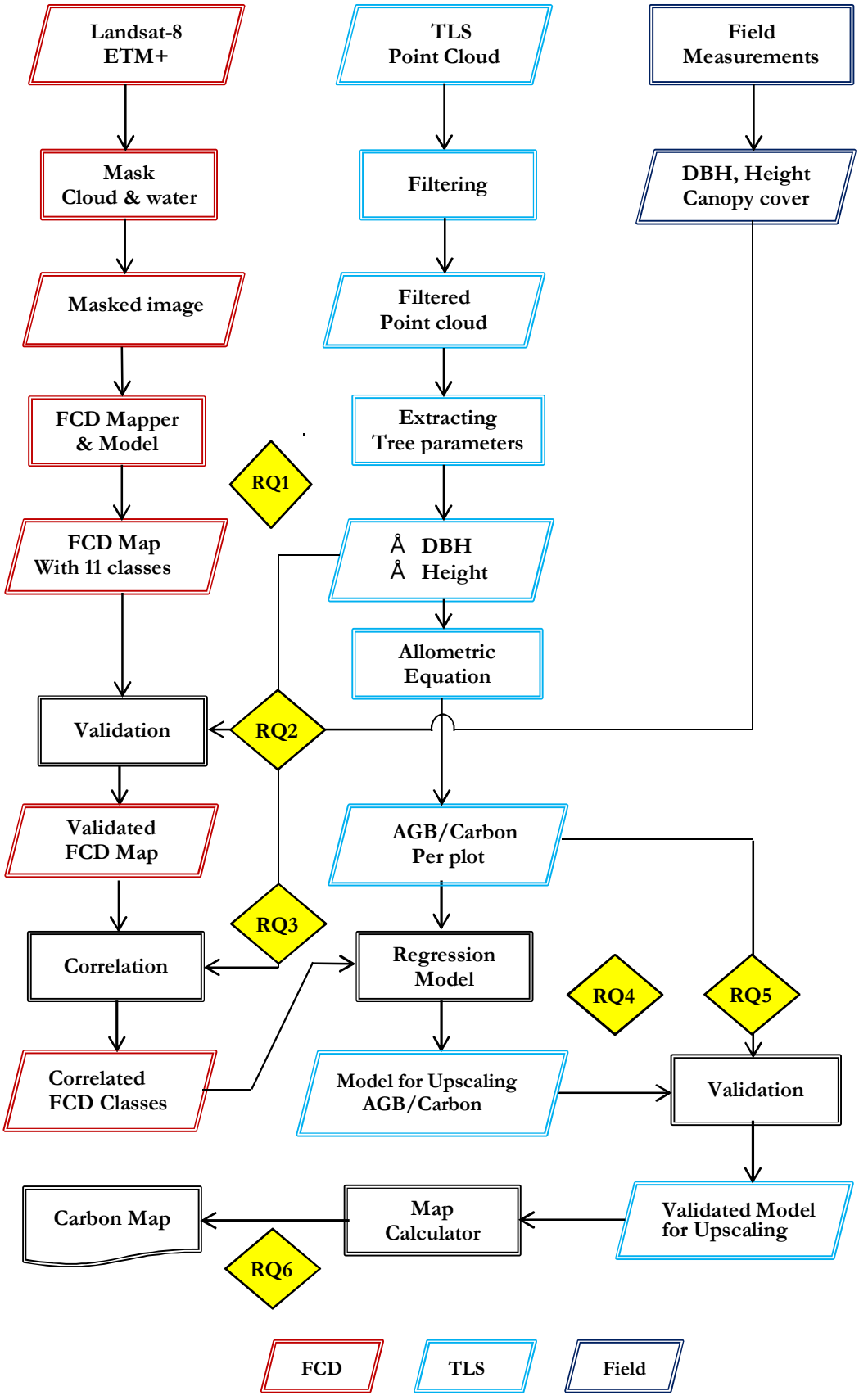

RQ= Research Question

Figure 10. Flow chart of research methodology

3.3.1 Pre field work stage

3.3.1.1 Radiometric and atmospheric correction

Correct interpretation of scientific information from remote-sensing product requires the ability to discriminate between product artefacts and changes in the Earth processes being monitored. Radiometric characterization and calibration is a prerequisite for creating high-quality science data and products (Roy et al., 2002). Then follows step in pre-processing the image to mask cloud, cloud shadow and water. Unless they are corrected these effects have an adverse influence on the statistical treatment and analysis of imagery data (Rikimaru et al., 2002).

3.3.1.2 Geo-referencing

Remotely sensed image have no reference to a location. The image therefore must be geo-referenced to relate the scene of the image to reflect the surface of the study area (earth surface). Satellite images and aerial photos were geo-referenced before image classification (Panta & Kim, 2006).

3.3.1.3 FCD mapping

The FCD mapper is a computer software package contains algorithms and other formulas utilized to compute values of several indices contained in the FCD model for the analysis of Landsat imagery data (Rikimaru et al., 2002). According to Rikimaru (1997), the processes of FCD-mapper can be explained as follows:-

1. Create a new project

The process started by creating a project named Malaysia under the expert name dialog box with file position, author and comment was created. The expert file contains all the information the FCD mapper uses to manipulate the different Landsat TM bands to calculate all the indices used to get the final forest canopy density map.

2. Image import

Image subset of the study area from the Landsat-8 ETM+ prepared was imported. Each of the seven bands were imported to the software to start processing of the images in the FCD mapper. This step was careful undertaken in order to use the right band. This step transforms the TIFF type of file to FBI files where it can be recognized by the software.

3. Opening & displaying images

Shadow index (SI) was derived from each visible band low irradiance area. But this low irradiance data may confuse shadow phenomena was avoided by overlaying thermal index (TI). Black soil have high temperature due to its high absorption while shadow lead to a decrease in soil temperature.

4. Noise reduction and normalization

All the data had been adjusted to conform to a common standard. Variations in shade on different parts of image were normalized. Then, the water set was used to identify area using a histogram to set the value for masking the surface water.

5. Calculation of vegetation and bare soil index

For calculating VI, PCA was selected to calculate the VI in the form of NDVI.

6. Calculation of thermal index (TI)

In the software false select windows was applied to visualize the areas with high and low TL. Area with high TI displayed as very light area and vice versa.

7. Calculation of shadow index (SI)

The shadow index is a relative value. The SSI is normalized value to integrate VI value and SI values. There is a directly relationship between SSI value and forest shadow value. Using the SSI it was observed that the vegetation in the canopy and vegetation on the ground could be clearly differentiated.

8. Vegetation density (VD)

This index used to separate vegetation from non-vegetation area by setting the minimum and maximum threshold for VI.

9. Scaled shadow index (SSI)

In this process the study area was classified into clusters using VI, BI, SI and TI images. After the forest area was identified, the range of SI was adjusted to fit between 0 to 100%. This was called as scaled shadow index.

10. The process of integration (SSI and VD)

The forest canopy density (FCD) value transformed the integrated of VD and SSI indices. Since the two parameters had dimension and percentage scale unit of density, it was possible to synthesize both indices by means of corresponding scale and unit of each indices.

$FCD = (VD+SSI+1)^{½} - 1$

From this FCD model 11 classes were generated. Then the accuracy of the model was verified using field data.

According to Azizi et al. (2008) results of previous studies in the Iran concerning to characterization of forest condition using FCD model shows 0.84 correlation with field data. It indicates higher correlation and accuracy compared to conventional remote sensing method. Similarly, Chandrashekhar et al. (2005) and Joshi et al. (2006) result demonstrate the model lucrative accuracy more than other method to classify forest density.

3.3.2 Field Work for Data Collection

To verify the FCD Mapper 11 classes generated, ground truthing plots are required to compare the canopy density figures (Rikimaru & Miyatake, 2002; Mon et al., 2012). Purposive sampling, a type of non-probability sampling technique was used. Purposive sampling is the proper one to use because it will evenly represent all existing classes. Inventory data from field plots have been the most practical means for estimating AGB (Brown, 2002). A reasonable number of sample of 3-5 plots for each class, were taken to ensure representation of 11 FCD classes. Representative plots were identified and their x and y coordinates were uploaded to iPAQ.

1. Sampling Design

Purposive sampling design was used to identify sampling points for ground truth of FCD map generated classes. A purposive sampling design was chosen to get representation of all the classes exist in the study area (Breidenbach, 2010). FCD Mapper is suitable to estimate forest canopy density in areas where collecting large amounts of field data is difficult because of inaccessibility or resource insufficiency (Mon et al., 2012). The sample size is often be a compromise between the desirability for more data and the cost of making measurements (IPCC, 2006a). The study area is inaccessible and untapped forest. Two data sets; which are biometric data from manual tree parameters measurement and point cloud data from TLS scanning were collected. Especially TLS scanning takes time compared to conventional forest mensuration and on average only three plots can be scanned using multiple scanning per day. During the field work data of 32 plots which represent 7 classes were collected.

2. Biometric data

The sampling unit of a circular plot with 12.62 m radius was delineated in the forest. Circular plot is widely used since it needs only as a single dimension, i.e. radius. This makes it easy to define and measure in the forest and has minimum perimeter for the given area without predetermined orientation and lowest number of borderline for tree selection (Husch et al., 2002). The radius can be changed with slope. In some of the plots slope correction table was used to define the radius with respect to the slope. Trees with

DBH 10 cm or greater within the plot were only measured as trees less than 10 cm diameter contribute little to the biomass carbon of a forest (Brown, 2002). Numbering of the trees with DBH more than 10 cm was done by putting post on the trees. Measurement of tree DBH using diameter tape, tree height using laser ranger finder, crown diameter using measuring tape and plot wise crown cover density using hemispherical camera was carried out.

3. TLS scanning

Generally, TLS scanning is conducted after manual measurement to avoid movement of people during scanning process. Since it takes quite a long time than manual measurement, it can also be carried out along with manual measurement to save time. For each plot four (4) scan position (multiple scan) where one is in the center of the plot and three around and just outside (i.e., 3 m far from the boundary of the plot) were taken. The steps used for scanning are listed as follows:

- **Identification of plot center and numbering of trees**

The scanning process starts first by identifying the center of the plot. Since prior to TLS scanning manual measurement was conducted the center of the plot was already marked. Then, followed by numbering of trees using laminated posts bearing number's facing to the center of the plot. The posts can be wrapped up around the tree using plastic tape or nails to place the post on the bark of the tree (Figure 11). This is very helpful in identification of trees during individual tree extraction from point cloud data.

Figure 11. Numbering of tree using post

- **Setting tripod**

Tripod set where the TLS instruments is mounted in the center of the plot (Figure 12). The instrument is equipped with inclination sensors which indicate boresight misalignment. The instrument offers a procedure to check misalignment error by means of calculating the roll, pitch and yaw angles. The angles will be calculated in to orientation values to be adjusted until optimal value is reached. It is advisable to have two tripods. This is important due to the fact that it will save time once the second tripod is set ahead for the next scan position. Whilst, every time the tripod will be removed from the previous scan position and will be carried along with the instrument to the next scan positions.

Figure 12. Setting TLS on a tripod

- **Setting TLS**

The TLS setting involves selecting a new project and set scan for the form and pattern of scanning, camera setting and inclination (pitch, yaw & roll) value. Moreover, the range of scanning can be selected. The range was changed from 100 to 50 m to reduce time spend in scanning and save space for storage data. For every scan, a range form and full wave form scan was made. In the range form scanning panorama 60 form of pattern was used. The reflectance setting of amplitude reading for detection threshold of the instrument of 0.05 decibel (dB) and, cylindrical and circular tie points were used.

- **Setting three scan positions**

Three outside scan position with an angular difference of 120^0 in between the scan positions was measured and the positions were marked (Figure 13). In the study the outer scan position were 3 m far from the boundary of the plot were used.

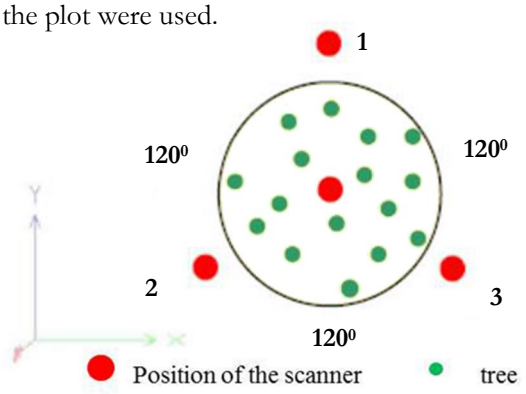

Figure 13. Setting the scan positions

- **Setting tie points**

When the scan position identified 4 cylindrical tie points along the line of sight of each scan position with a total of 12 cylindrical (with 10 cm in diameter and 10 cm length) and 4 additional circular, in total 16 tie points were used during scanning process (Figure 14). The tie points should be visible from the two ends; which the center and the three outer scan positions. In most of the plots minor clearing of leaves and twigs was carried out to clear the line of sight and placing the tie points on sticks (Wezyk, et al., 2007). When placing tie points they should not be aligned in a line, they need to be placed in a way that they form a rectangle to enhance tie points position during tie points marking and detection process. The four circular tie points were used as remarks and the 3D coordinates were taken using a total station. Having more tie points will take time especially during detecting individual tie points by the scanner, however it will maximize the number of tie points that might be blocked due to trees or part of tree during tie points scanning. This will guarantee the number of tie points needed for registration although a minimum of three tie points are required to register a scan (Simonse et al., 2003).

a)

b)

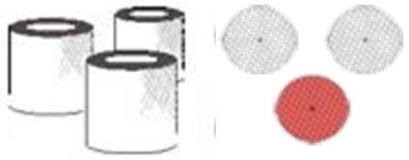

Figure 14. Tie points- a) Placing tie points in a plot b) tie points from Riegl (Bienert et al., 2006)

.

- **Image acquisition**

The Riegl VZ-400 is equipped with Nikon D610 mounted camera with 20 mm and 50 mm lens camera. After every scanning is completed automatically images are taken of the scanned area. The number of images could be set and 7 images per scan are sufficient. These images will then be used to colorize point cloud data for better visualization during processing.

4. Total station

The coordinates of the plots, scan position and tree positions were taken using total station GPS technique. RiSCAN PRO software allows adding externally the coordinates by creating new tie points to the different scan positions of the plots. This method of geo referencing point cloud could be connected to a total station (Simonse et al., 2003). The total station readings were taken by surveying team of University Technology Malaysia (UTM).

3.2.3 Post Field Work Stage

3.2.3.1 Cloud data processing for derivation of tree parameters

1. Registration

The first pre-processing step was to register the four scan positions (multiple scan) in to a common reference point. Registration will ensures the most complete 3D information about the trees. Then filtering was applied to the point cloud data to remove noise and clip the data to exclude trees outside the plot (Aschoff et al., 2004; Simonse et al., 2003). Filtering to 12.62 m was executed to exclude trees outside the plot. An example of a filtered plot is shown in Figure 15.

Figure 15. Filtered plot (Bienert et al., 2006)

2. Extraction of Trees

Trees with more than 10 cm DBH are the most important objects in the plot. Recognition of tree can be done automatically (Aschoff et al., 2004) or manually. Segmentation and tree identification can be done in a horizontal cut of point cloud data and automatic detection reduces time (Bienert et al., 2007). As it was indicated in the field data collection plot identification these trees were identified and numbered with posts. The numbering made the identifying trees with in the plot possible using RiSCAN PRO V1.8.1 software.

3. Extraction of tree height

Tree height is determined from the difference between the lowest point (Z-value) and the highest point inside the cut of cylinder (Hopkinson et al., 2004). After individual tree extraction from plot point cloud data completed. The individual tree point cloud data was exported to other programmes (e.g. MATLAB) and the height was generated (Figure 16).

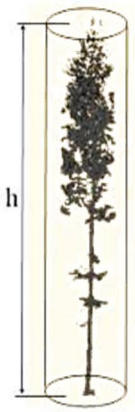

Figure 16. Tree height determination (Bienert et al., 2006)

4. Extraction of DBH

Determination of DBH is often done by fitting circle rings to all points situated in a layer 1.25 - 1.30 meters above the ground to the tree trunks. According to Thies et al. (2004) study made in forest inventory in Germany used manual DBH measurement from TLS data. The height of DBH measuring depends on the DTM, which might be an error source when comparing the results to the field measured DBH. According to Watt & Donoghue (2005) found an average difference of 1.5 cm in DBH measurements between TLS and field measurement.

3.2.3.2 FCD Map validation

To verify the accuracy of the density maps, ground truthing was carried out by comparing the crown density figures produced by the FCD software with direct field observations. Correlation analysis between FCD map and field measured was used (Rana & Vickers, 2005). Similarly, Baynes (2004) used correlation to verify the accuracy of the FCD map of the landscapes in Australia and Philippines.

3.2.3.3 AGB/Carbon estimation

Carbon stocks and their changes of the biomass pool can be estimated from forest inventory data by using either biomass equations (BE) or biomass expansion factors (BEF) and conversion factors (i.e. wood density) (IPCC, 2006b). Allometric equations were used to estimate AGB/carbon. To calculate AGB since there no site specific equation for the tree species in the study area, a generalized allometric equation developed by Chave et al. (2005) was used. The equation is given as follows:

$$AGB = 0.0509 \times \rho D^2 H \quad \text{..... (Equation 1)}$$

Where,

AGB = above ground biomass [kg]
ρ = wood specific gravity [Kg/m^3]
D = tree diameter at breast height (DBH) [cm] and
H = tree height [m]

Wood specific gravity for used species is used from the study made in Malaysia (King et al., 2005). Then carbon stock was calculated from AGB conversion factor 0.47(IPCC, 2006a)

$$\text{Carbon stock} = 0.47 \times AGB \quad \text{..... (Equation 2)}$$

3.2.3.4 Correlation analysis

Pearson correlation coefficient, also known as r, R, or Pearson's r, is a measure of the strength and direction of the linear relationship between two variables (Reimann et al., 2011).

$$r = \frac{\sum_{i=1}^{n} (X_i - \overline{X}) - (Y_i - \overline{Y})}{\sqrt{\sum_{i=1}^{n} (X_i - \overline{X})^2} \sqrt{\sum_{i=1}^{n} (Y_i - \overline{Y})^2}} \quad \text{..... (Equation 3)}$$

The closer r is to +1 or -1 the stronger the positive/negative correlation is. If the correlation coefficient (r) is equal to 1 exactly, the two variables are perfectly correlated. Generally, the correlation coefficient value of >0.70 or <-0.70 is usually considered as a strong relationship between variables (Reimann et al., 2011).

3.2.3.5 Regression analysis and model validation

Regression analysis has intensively been carried out for modelling the relationship between remotely sensed data and field measurements with the objective to quantify the relationship between the dependent variable and one or more independent variable. Correlation coefficient (r), coefficient of determination (R^2) and root mean square error (RMSE) were calculated which shows the percentage of variation in one variable which associated to that variables. The R^2 and RMSE are used to evaluate model performances. These two methods are important since R^2 shows how much a model can explain and RMSE indicate the error in calculating estimates of the model. According to Lu (2006) a model with high R^2 and low RMSE value indicate the goodness of fit. In this study, RMSE gives error in Kg. RMSE is calculated using the formula listed as follows:

$$\mathbf{RMSE} = \sqrt{\frac{1}{n}\sum_{i=1}^{n}(C_p - C_o)^2} \qquad \text{…….. (Equation 4)}$$

Where,

C_O = Observed carbon

C_p = Predicted carbon

n = Number of observations

RMSE is expressed in percentage, which is calculated from the ratio of RMSE and average observed carbon.

3.2.3.6 Carbon Mapping

A regression model was developed and validated once the regression analysis was accomplished. The model was used to estimate the AGB and carbon stocks of the study area. To achieve this, above ground biomass and carbon stock maps were generated.

4. RESULTS

4.1. Descriptive statistics of TLS data

From 32 purposive sample plots 30 plots of forest stand parameters (i.e., height and DBH) measurements of field and TLS point cloud data were collected. The two plots were excluded since trees were not able to be extracted from the plot level TLS data. From the 30 plots 604 field measured forest stand parameters (i.e., height and DBH) and 601 from TLS tress parameters measurement were used (see Appendix 3). Descriptive statistics were used to explore, summarize and present the data. The descriptive statistics are presented in two sections as distribution of species and measurements of the tree parameters.

4.1.1. Distribution of species

There are 52 tree species found from 604 trees field measurement. Among them, 15 species were recognized as dominant species and the other species categorized in to one group named as "others". Besides the five *Shorea spp.* are grouped in to one large Shorea group. The descriptive statistics of total 604 trees sample are visualized in Figure 17 shows the detailed distribution of species.

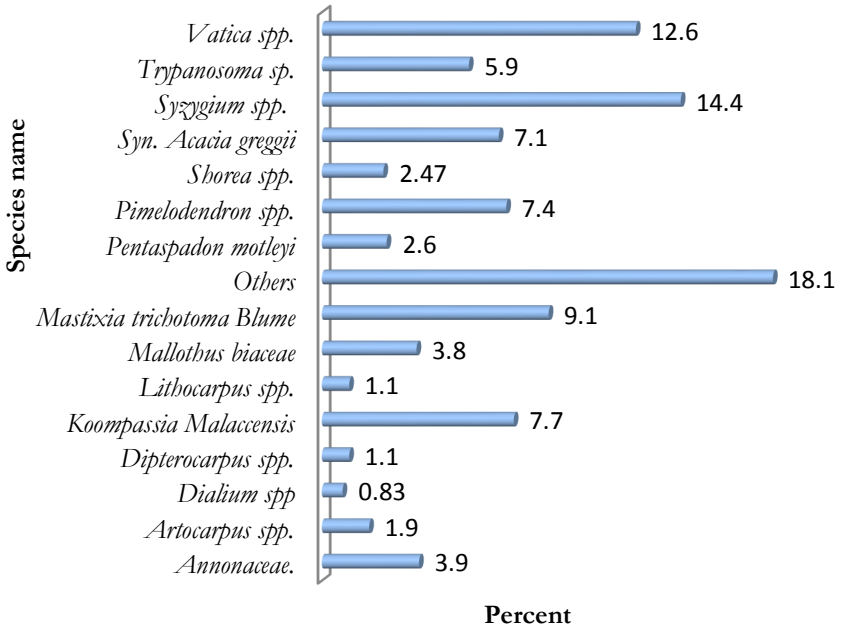

Figure 17. Bar graph distribution of 15 species (from 100%) found in the study area

4.1.2. Tree parameter measurements of TLS data

From the TLS measured tree parameters, 601 trees (excluding 3 incomplete observations from 604) DBH and heights were measured for trees in 30 plots. Descriptive statistics of total 601 trees sample shows that diameter and height of the trees sampled range from 10 to 110 cm and 4.95 to 40 m respectively. The summary of the descriptive statistics are presented in Table 4.

Table 4. Descriptive statistics of 601 TLS trees parameter measurements

Variable	Min	Max	Mean	Standard Deviation	Skewness	Standard error	Kurtosis	Standard error
DBH	10.0	111.20	22.74	16.01	2.556	.100	7.716	.199
Height	4.95	40.25	15.13	5.88	1.291	.100	2.058	.199

Box Plot of DBH and height shows the full range of variation between minimum and maximum value (Figure 18). There is wide variation in DBH as compared to height. As is shown in the table, the mean of tree diameter is 22.7 cm and height is 15 m with considerable observation of outliers.

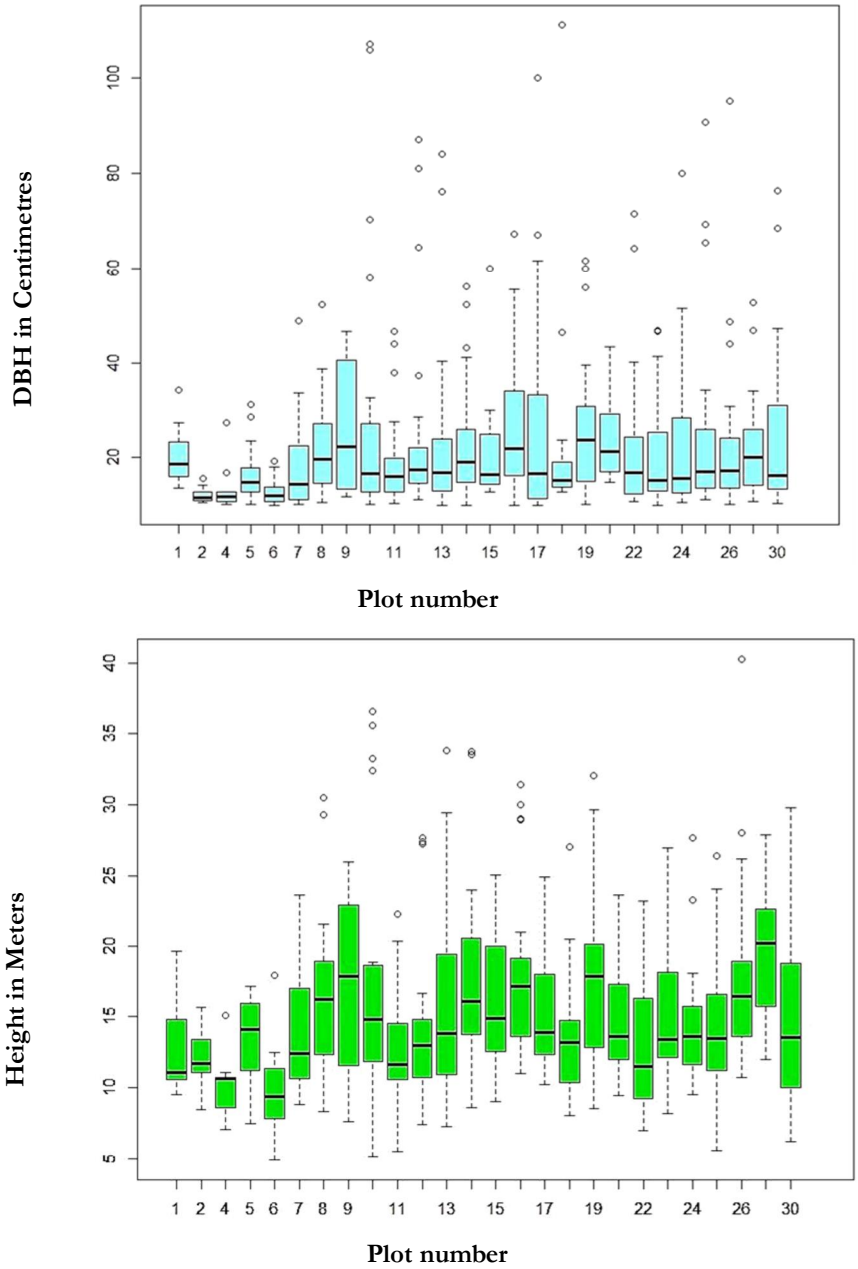

Figure 18. Box plot of DBH and height of trees distribution in 30 plots

The normality test was carried out to determine the normality of the data. Normality of the samples is calculated based on skewness and kurtosis of the data. It combines skewness and kurtosis into a statistic overall test. skewness measures the extent and direction of symmetry or asymmetry of the distribution whereas Kurtosis peakedness of the distribution and the thinness or thickness of tails in the distribution. The skewness and kutosis value is shown in Table 4 and Figure 19, the skewness is considerably high to the left (positive skew) for the both variable which implies that distribution of the data of diameter and height of trees is not normal. Normality test indicates the distribution of data in both variables is non-normal (Appendix 5). However, data below 10 cm DBH were not collected.

Therefore, the skweness is present, otherwise both DBH and height would be more normal if data below 10 cm DBH have been collected.

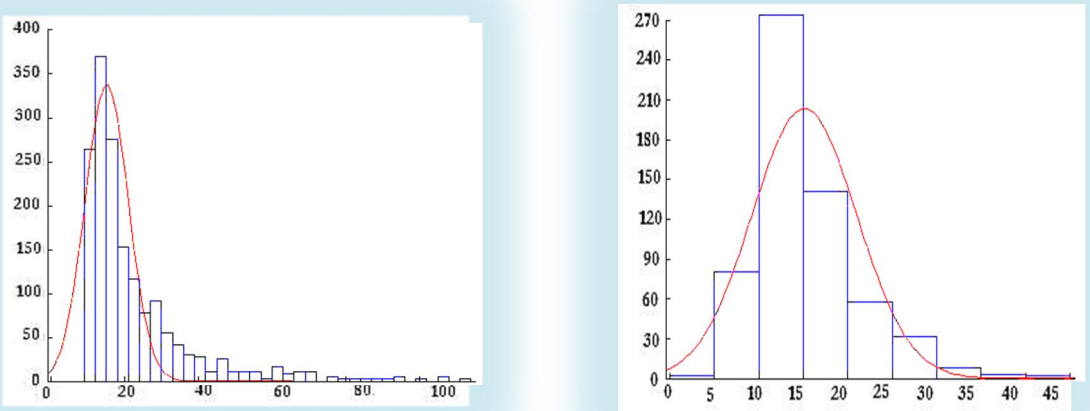

Distribution of DBH Distribution of height

Figure 19. Distribution of DBH and height of trees

4.2. FCD mapping

4.2.1 FCD classes

The FCD mapper and model produces 11 classes (10 canopy classes and one non-canopy class) and the 10 canopy classes (1– 100) are presented with intervals of 10 percent. The total area classified is 3,442 Ha, out of this 34.5% is covered by water and the remaining 65.5% by forest. The FCD map is shown in Figure 20.

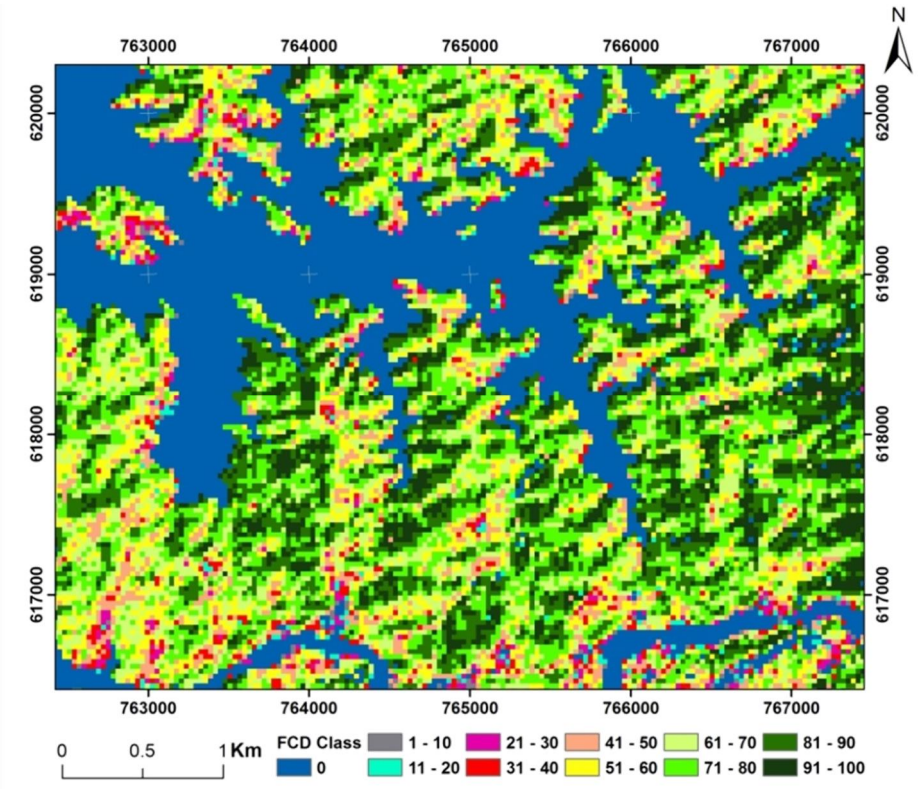

Figure 20. FCD map of the study area

4.2.2 Distribution of FCD classes

The distribution of the canopy density classes in the study area is summarized and presented in the Figure 21. The figure shows the area (Ha) per class and percentage share of each class out of the total area in 100%. Among canopy classes, maximum area falls in class 8 and the smallest area in class 1. Class 7 second highest figure followed by class 9, class 6, class 10, class 5 and class 4. These seven classes make up 95% of the forest area.

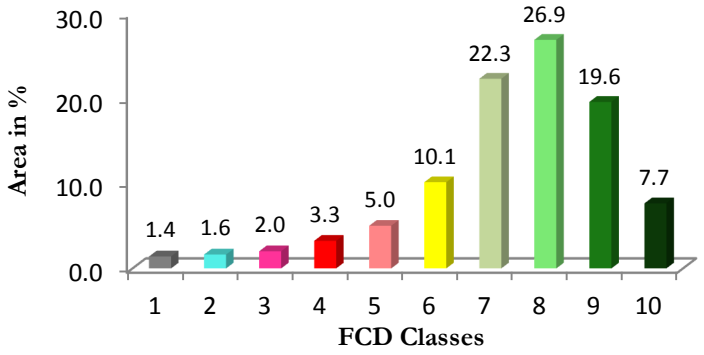

Figure 21. Class wise FCD area distribution in percentage

4.3. Validation of FCD map

To verify the accuracy of the canopy density maps, ground truthing was carried out by comparing the crown density figures produced by the FCD mapper software with direct field observations from classification of hemispherical photographs (see Appendix 9). The correlation between FCD map and field measurement was established and is presented in Figure 22. The result shows a strong correlation of 0.84 between FCD map and field measurements of the canopy density of the study area.

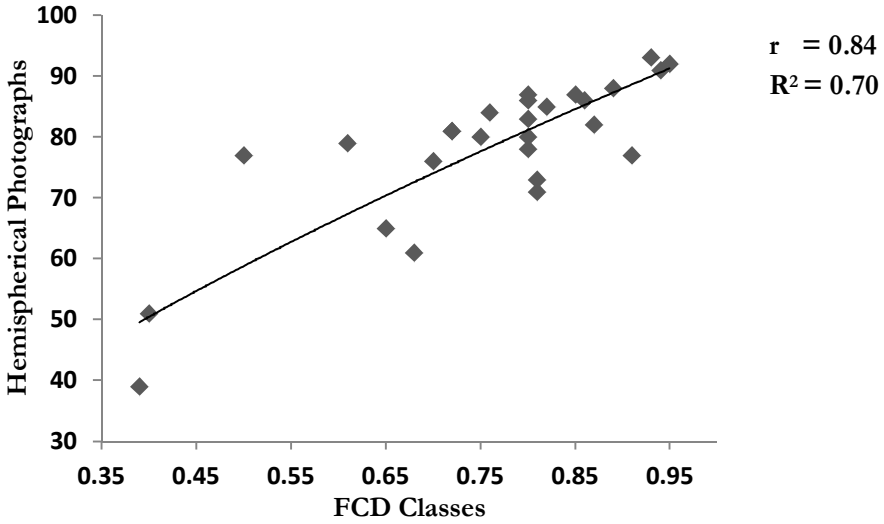

Figure 22. Scatter plot of relationship between FCD classes and hemispherical photographs

4.4. Point cloud data

4.4.1 Registration

The four scans (one in the center & three outer) are recognized as standalone scans and are not aligned when visualized before registration. Registration is done then to integrate the multiple scans using one reference point. The tie points were used to transform the four individual scan to a referenced point

which is the center scan. The registration process was carried out using the software RiSCAN PRO for the 32 plot with minimum and maximum range or 1.01 to 4.21 cm. Figure 23 visualizes the alignment of the four scans after registration (see Appendix 8). In line with registration, geo referencing was also carried out by adding coordinates from total station readings externally to the scans.

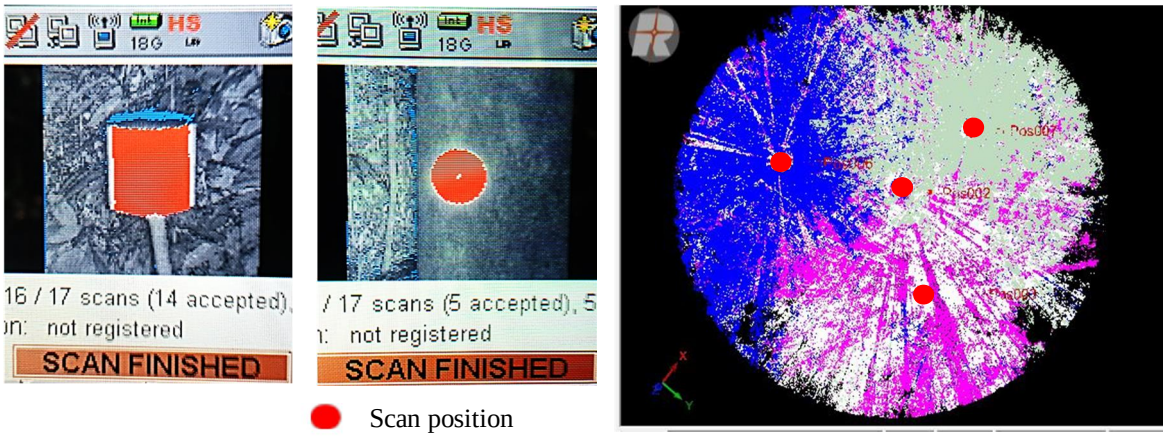

Figure 23. Registration- a) tie point detection b) registered multiple scans

4.4.2 Tree extration

Trees with more than 10 cm DBH are the most important in the plot. Recognition of tree can be done using different view types of RiSCAN PRO, Figure 24 shows the colorized (RGB) mode point cloud data. Numbering of tress with post enhance recognition of trees inside the plot. Tree identified where sliced from plot level point cloud data and stored in a form of polydata for individual tree. From 698 trees of the 30 plots, 604 trees were extracted from the multiple scan point data. The result shows missing of 94 trees, which accounts to 86.5 % detection rate was able to be covered by multiple scans.

Figure 24. Tree extracted from plot wise colorized point cloud data

4.4.3 Extraction of tree height

After individual tree extraction from plot point cloud data was completed. Tree height was determined from the difference between the lowest point (Z-value) and the highest point of the sliced individual tree point cloud data. The individual tree point cloud data was exported to other programmes (e.g. MATLAB) and the height was generated from the difference as portrayed in Figure 25. Tree height of 601 trees was determined.

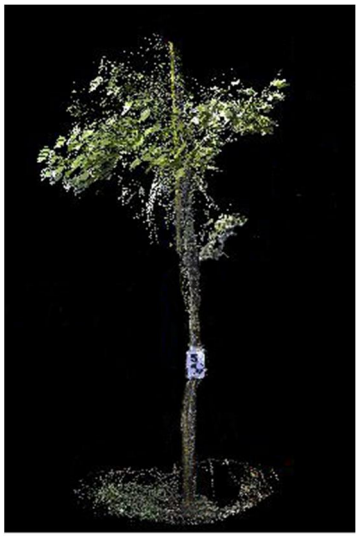

Figure 25. Extracting tree height from point cloud data

4.4.4 Extraction of DBH

Determination of DBH is often done by fitting circle rings to all points situated in a layer 1.30 meters above the ground to the tree trunks. Every tree 1.30 meters above ground was marked and measured as illustrated in Figure 26. Then, DBH was determined by measuring the distance manually. DBH measurement for 604 trees was performed.

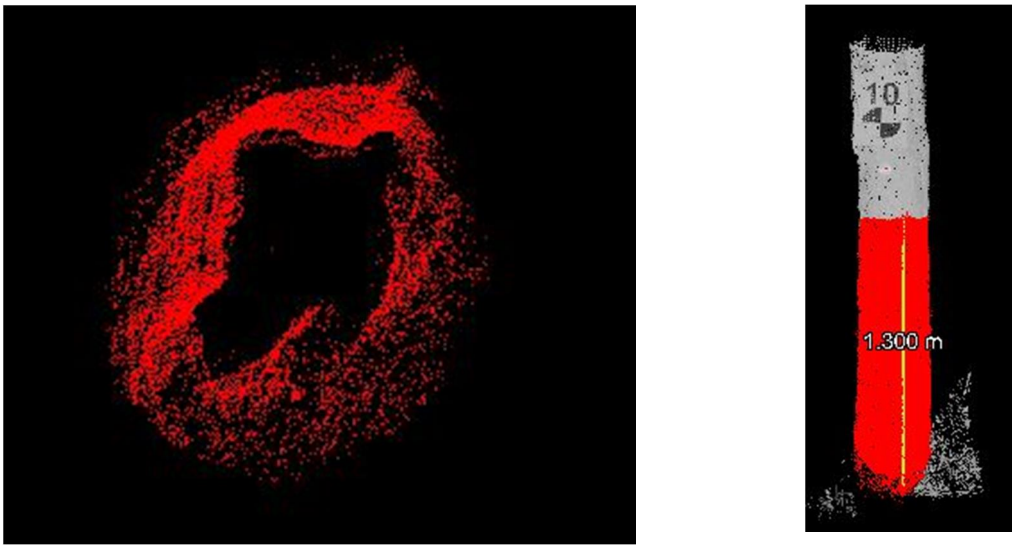

Figure 26. Extracting DBH of a tree from point cloud data

4.5. Relationship of FCD with TLS parameters

Once the TLS parameters (DBH & height) are obtained their relationship with FCD classes need to be examined. Since FCD indicates surface area, single dimension of tree could not be directly correlated. Thus, basal area from DBH had to be calculated for trees inside the plot. Plot level basal area was correlated to FCD classes to assess the relationship. A scatter diagram of two variables was established in Figure 27 in order to assess the relationship between FCD and basal area. A strong relationship between the two variables is observed.

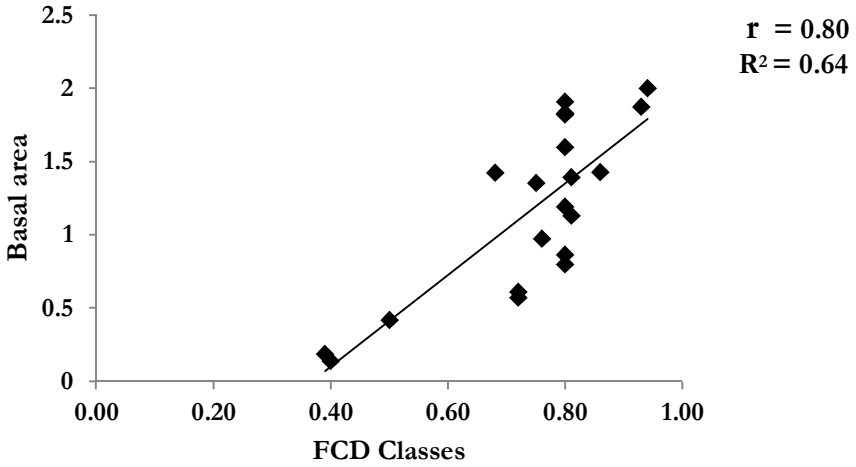

Figure 27. Scatter plot of relationship between FCD classes and basal area

4.6. Relationship of FCD with Biomass/carbon

Prior to developing a model for biomass prediction, a relationship between biomass of the plots, which was calculated using IPCC 2006 recommended allometric equation from TLS measured tree parameters (DBH and height) and FCD classes had to be examined. Log transformation was performed, since DBH and height variables were not normally distributed. Then biomass of the plots was calculated using Chave's allometric equation. A scatter diagram of the two variables was portrayed in Figure 28 in order to see the relationship between biomass and FCD. Correlation coefficient and coefficient of determination (R2) was calculated. This shows the percentage of variation in one variable associated to the other variables and can be explained using a regression equation.

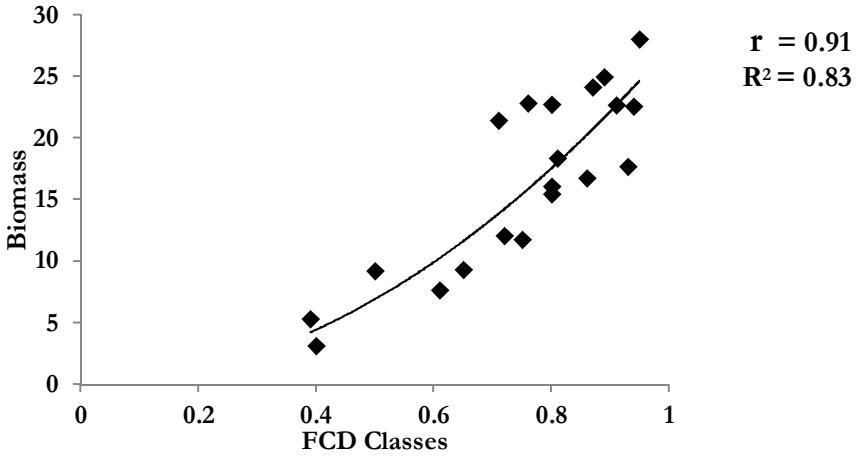

Figure 28. Scatter plot of relationship between FCD classes and biomass

4.7. Regression analysis

4.7.1 Model Development

To develop a biomass estimation model, variables FCD was used as a predictor. Analysis of the correlations coefficient among variables (DBH & height) was done in the previous (FCD & TLS parameters) which resulted in a strong relationship of those variables with independent variable FCD. Correlation between AGB prediction model and Observed AGB was developed to observe the relationship. Observed and predicted AGB were plotted against each other is illustrated in Figure 29 and R^2 was calculated to see the goodness of fit (Figure 29). The model developed expresses 66% of the observations and with 22% error in prediction of AGB.

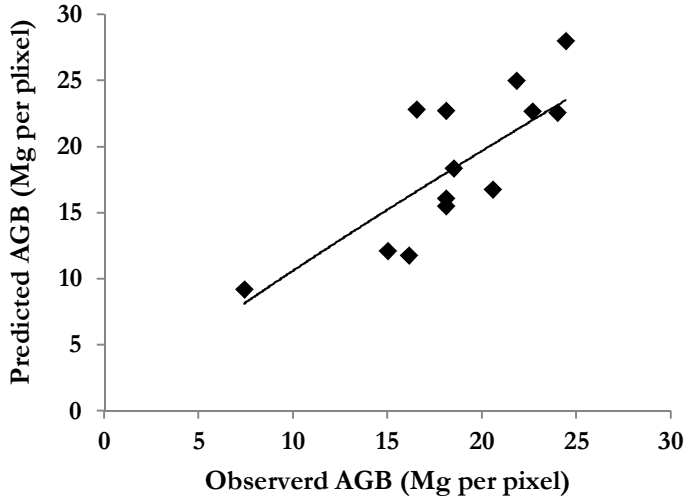

Summary of fit

Correlation coefficient	0.79
R square	0.66
Adjusted R square	0.61
RMSE	0.22
Intercept	1.37
Power	0.89
Observation	13

Figure 29. Summary of fit the regression model

4.7.2 Model validation

Models with higher adjusted R^2 and low RMSE are indicative of reasonable predictive ability of biomass. The model developed resulted with R^2 value of 0.66, meaning 66% of observations can be explained by this model. The model was validated using randomly selected 7 independent sample plots (35% of the data), then the AGB was upscaled to a pixel size (900 m^2). When the model was validated the R^2 value increased to 73%. The results of the summary of fit are presented in Figure 30.

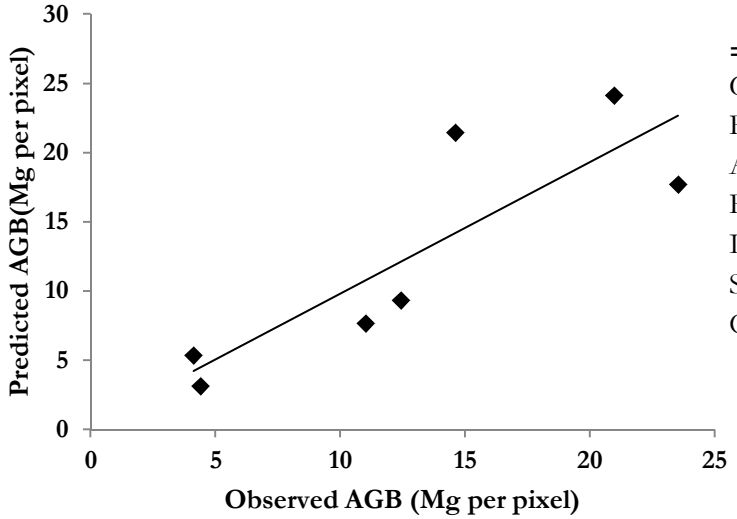

Summary of fit

Correlation coefficient	0.85
R square	0.73
Adjusted R square	0.67
RMSE	0.31
Intercept	0.95
Slope	0.34
Observation	7

Figure 30. Summary of fit the regression model

4.8. AGB and carbon stock mapping

4.8.1 AGB mapping

The AGB map of the study area was generated from the regression model that was validated. The result of AGB map is visualized in Figure 31. The average biomass was estimated in tons/ha in the study area which means about 344 $MgHa^{-1}$ of biomass. The summary of the calculation is listed in Table 5.

Table 5. Summary of the average and total biomass calculation in the study area

Average biomass per plot in Kg	Average biomass per Ha in Mg	Average Carbon per plot in Kg	Average Carbon per Ha in Mg	Total Biomass Mg	Total Carbon Mg
18233.24	344.19	8569.62	161.77	1184701.6	556809.75

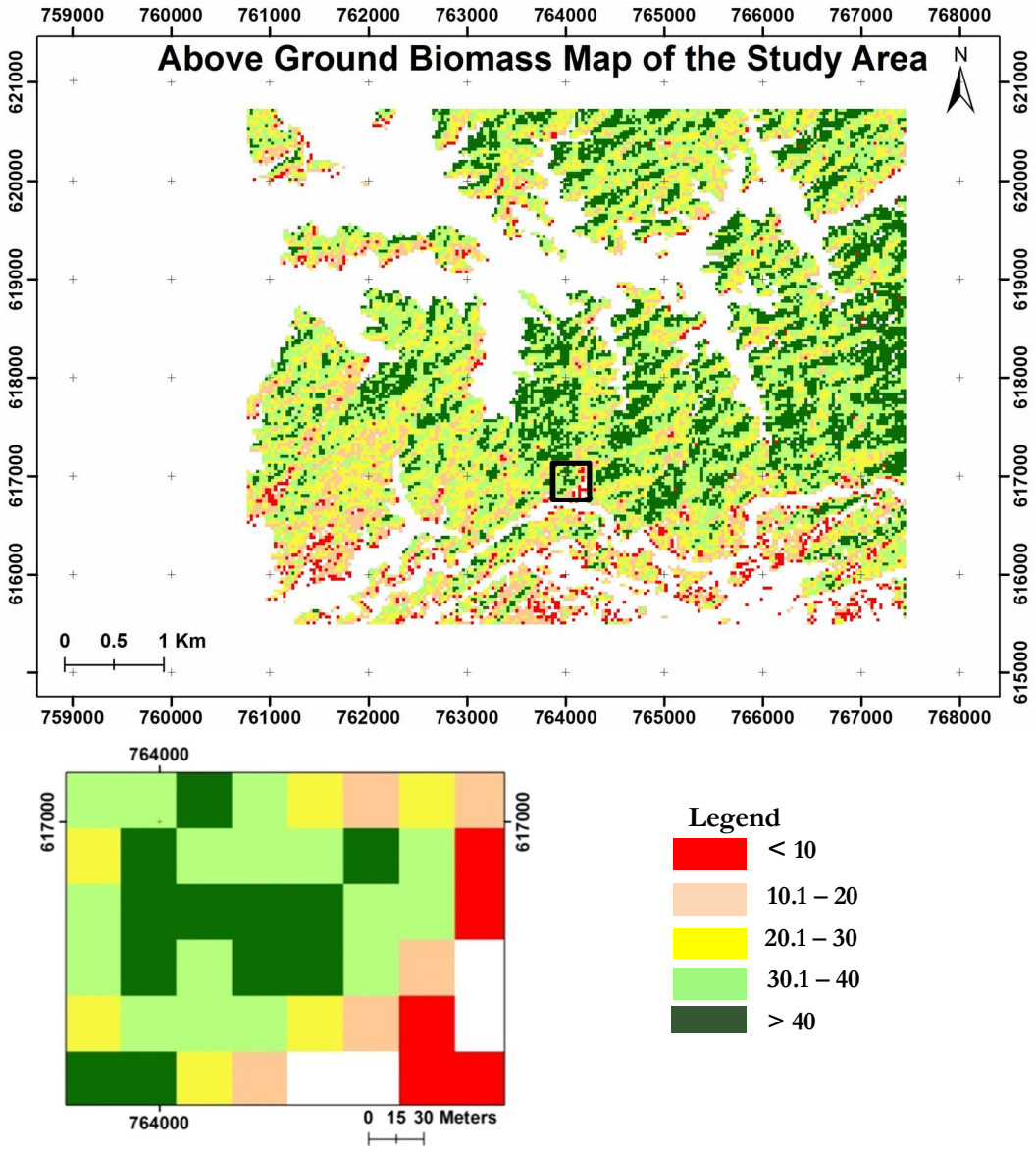

Figure 31. Above ground biomass map of the study area in Mg per pixel

4.8.2 Carbon mapping

As indicated in Table 8 above, the study area has approximately an average 162 $MgHa^{-1}$ of Carbon stock. The carbon map produced shows the stocking in Figure 32. In the figure, shows the details of carbon stock per pixel. The amount of carbon per pixel varies from less than 5 Mg per pixel to more than 20 Mg per pixel.

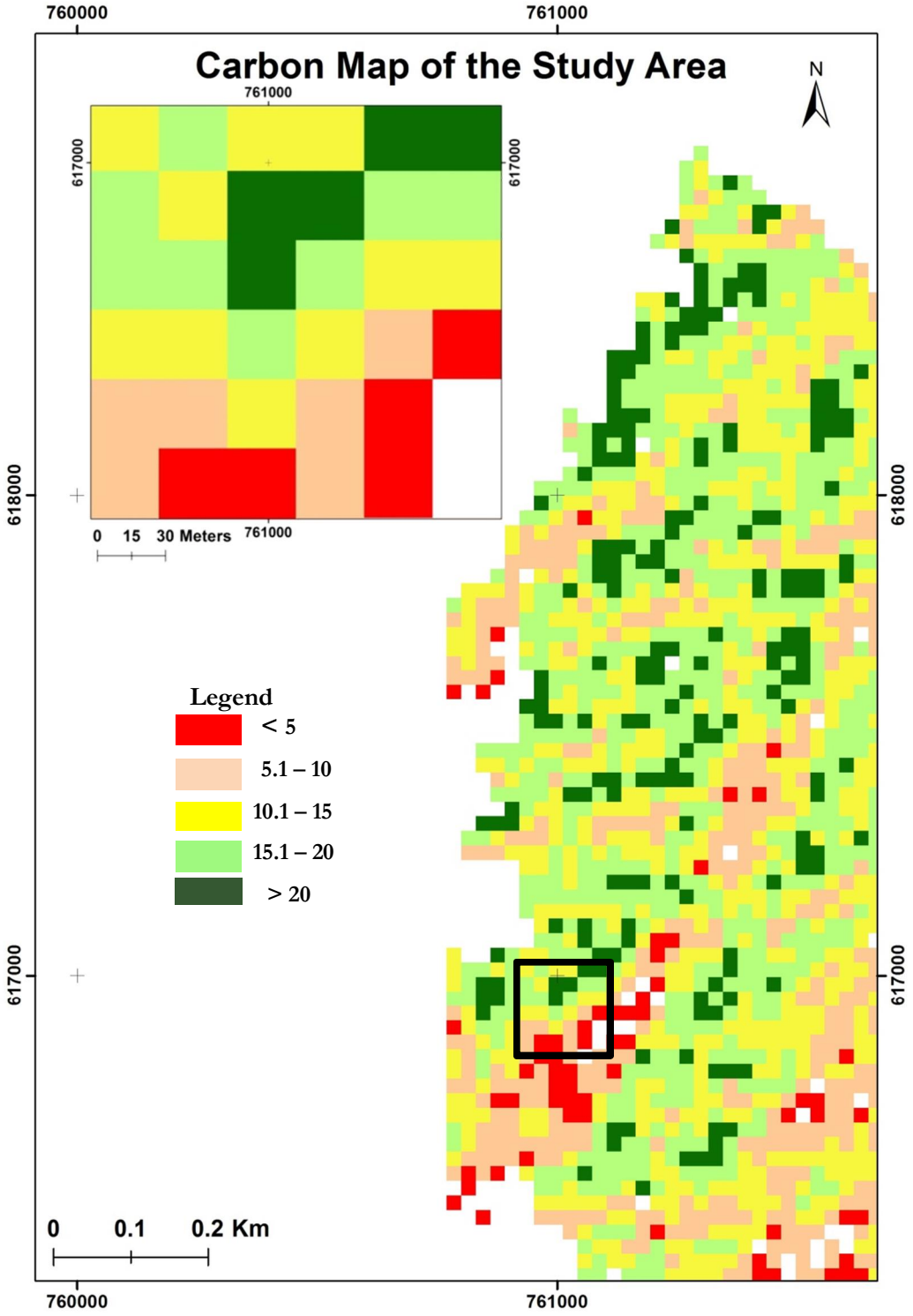

Figure 32. Carbon map of the study area in Mg per pixel

5. DISCUSSIONS

5.1. TLS parameters data

DBH and height features of 601 trees obtained from TLS point cloud data showed a non-normal distribution. DBH is highly skewed while height slightly skewed. Skewness quantifies the degree of symmetry of the distribution around the mean. The skewness value may be negative, positive or zero (Reimann et al., 2011). If a distribution is normal, the skewness value is 0. In the case of the 601 sample of trees diameter and height are skewed to the right or positive skew (Figure 33). The non-normal distribution of the data may be caused due to the fact that measurements of diameter less than 10 cm were not taken, and only trees with DBH > 10 cm were sampled. Similarly, in the case of height, newly emerging seedlings stand more than 4 m high and value below 4 m are not included in the distribution. In addition, the sampled plots represent various types of FCD classes. As there are differences in FCD classes, there is quite variations in DBH and height of trees (see Figure 18).

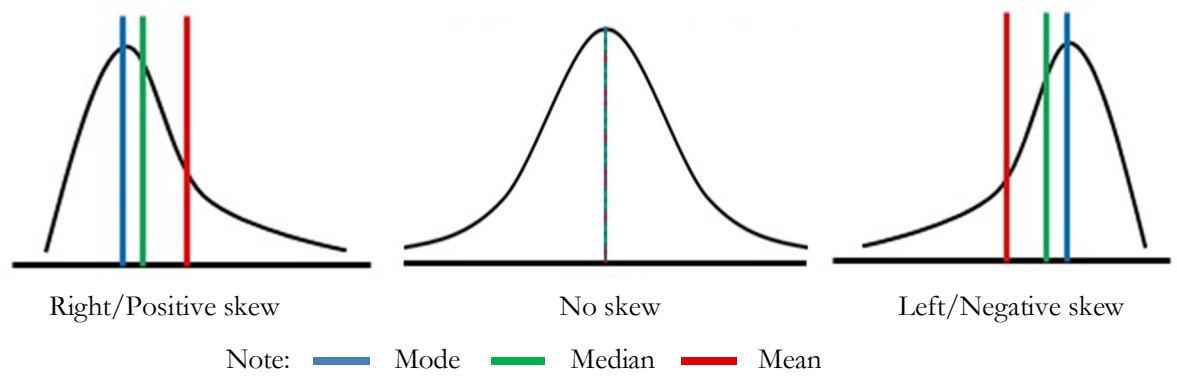

Figure 33. Illustration of the different types of distributions (www.whatilearned.wikia.com.)

5.2. FCD mapping

Findings of the study indicated that FCD mapper classified Landsat-8 ETM+ data in to 11 classes (one non-forest and 10 forest canopy classes) with intervals of 10 percent (see Figure 20). This shows that FCD mapper can classify Landsat-8 ETM+ data with relatively reasonable accuracy. This finding is consistent with results of other studies which showed high FCD mapping classification accuracy when compared with other image classification methods (Chandrashekhar et al., 2005; Joshi et al., 2006; Nandy, et al., 2003). Similarly, Mon et al. (2012) applied forest canopy density mapping satellite images classification to identify canopy openings which are useful parameter to monitor tropical forest. FCD mapper integration of biophysical indices attained from vegetation reflectance enabled it to acquire relatively high classification accuracy, when compared to other image classification approaches used in the afore mentioned studies, which consider only spectral reflectance.

As it is noted in the literature review FCD mapper and model use four indices namely: average vegetation index (AVI), bare soil index (BI), shadow index (SI) and thermal index (TI). The relationship between these four indices and FCD condition is explained in Table 6 (Rikimaru & Miyatake, 1997; Rikimaru et al., 2002). AVI increases as vegetation cover increases and it is observed to be high in forest and grass land. BI is a function of bare soil which increases with bareness of the ground and decreases with increments in vegetation. SI is high in forest areas, medium in grass land and low in bare land. To overcome underestimation of crown density in dense forest, where shadow cannot be sensed, SI is linearly transformed into scaled shadow index (SSI). Thus, SSI will correspond with the extent of the forest shadow. It starts at 0% with possible lowest shadow in forest and increases up to 100% in tropical forests with highest possible shadow. TI is negatively correlated with forest density. This is due to two main factors of the tropical forest, the blocking radiation and absorption of solar radiation on one hand and the cooling effect on the other hand as a result of evaporation from leaves (Baynes, 2004). SI and TI are combined to avoid misclassification of forest and bare soil, because shadow decreases soil temperature.

FCD mapper integrates all these indices to calculate vegetation density (VD). This will include forest and grass land while excluding bare soil. Separation of grass land from forest is carried out using an integration of SSI & VD, which is carried out to generate FCD map which shows FCD for each pixel (Baynes, 2004).

Table 6. Characterization of biophysical indices to contribution of different intensities of FCD

	High FCD	Low-FCD	Grass land	Bare Land
AVI	High	Medium	High	Low
BI	Low	Low	Low	High
SI	High	Medium	Low	Low
TI	Low	Medium	Medium	High

Note: High FCD Medium FCD Low FCD

The process of integration of the biophysical indices can be shortly summarized in the flow chart presented below.

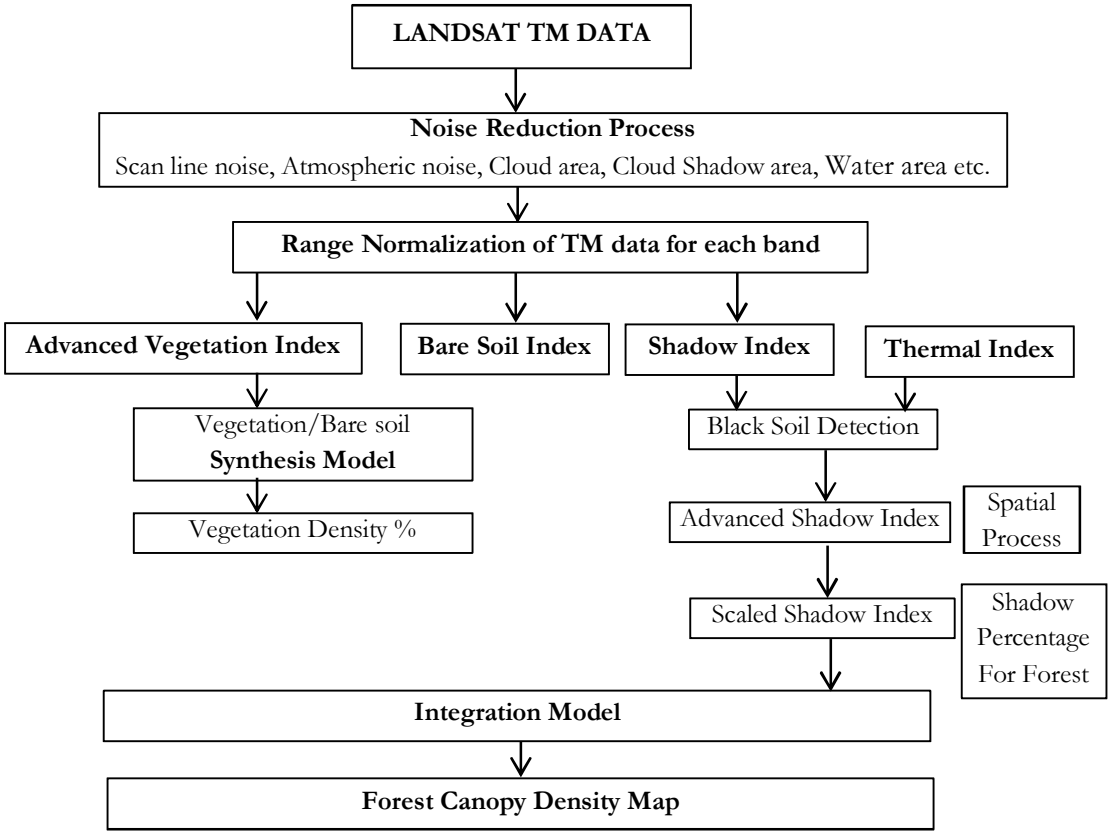

Figure 34. Flow chart of FCD mapping model (Rikimaru et al., 2002)

Besides the FCD map, the model also quantified the area allocated to the different FCD classes. The result revealed a total area of 2,237 hectares of land which accounts 65% of the study area that represent the 10 FCD classes (see Figure 21). Findings of the study concur with the designation made by Rikimaru et al. (2002) to FCD mapper and model as quantitative analysis to compute area of the canopy classes. This is the advantage of FCD over conventional remote sensing to estimate crown coverage or forest canopy cover based on qualitative data analysis derived from "training areas" with high cost requirements and time required for the establishment of training areas. The detailed analysis will add depth information in forest stand to analyze the growth, degree of degradation and the condition of the forest in general, each of which can assist foresters to assess and monitor the forest stand conditions.

5.3. Validation of FCD map

FCD model requires less information of ground truth for validation (Rikimaru & Miyatake, 1997). Mon et al. (2012) also noted suitability of FCD mapper in areas where there is difficulty in collecting large amounts of field data due to inaccessibility. To this verifying the accuracy of the FCD maps can be carried with less ground truth information using correlation analysis. Thus verification of the canopy density map of the study area was carried out by comparing the crown density figures produced by the FCD mapper software with direct field observations. As indicated in Figure 22, the analysis for this study revealed a high correlation coefficient value of 0.84 or R^2 0.70 between FCD map and ground truth information derived from hemispherical photographs. The high correlation coefficient value indicates the high degree of compatibility between FCD map and ground truth. Previous studies carried out by Roy et al. (1997) in evergreen and dry forest of India discovered a correlation coefficient value of 0.9. Rana & Vickers (2005) also revealed the result of 0.6 correlation coefficient value between FCD map and field measurement of crown density with densiometer. Similarly, Baynes (2004) used correlation to check the accuracy of FCD classification between FCD map and field measurements, although in that particular case, the analysis was not disclosed. In addition to this, Jamalabad & Abkar (2004) applied correlation analysis and found correlation coefficient value of 0.83. The results of these studies are similar to the findings of this study. The high correlation coefficient value indicates the high degree of agreement between the FCD map and the ground truth.

5.4. Attributes of FCD mapper and model

FCD mapper and model was developed as an alternative tool for mapping and monitoring changes in forest cover in tropics. The model has attributes that include: the use of Landsat satellite images to identify canopy openings which is a useful parameter for estimation of growing biomass/carbon stocks of forests. Landsat satellite images are free and can be used for monitoring large scale over time (Achard et al., 2004). Assessments of relative performance of different image classification approaches, for example maximum likelihood, image segmentation and multiple linear regression indicated that FCD mapper generated relatively higher accuracy (Chandrashekhar et al., 2005; Mon et al., 2012). In addition to this, FCD mapper uses an approach of quantitative analysis to express the area coverage of FCD classes (Rikimaru et al., 2002). Furthermore, it is robust and instantly derives an FCD map from satellite images. Finally, FCD mapper is inexpensive, technically easy to use and does not require specialized expertise. Therefore, FCD mapper is a very useful tool for tropical forest monitoring (Baynes, 2004; Mon et al., 2012; Rikimaru et al., 2002).

Finding of this study also revealed the fact that the model is a useful tool for estimation of biomass/carbon. As it is mentioned in the literature review, with all the above specified attributes FCD mapper and model can be used for estimation of biomass/carbon to meet MRV mechanisms of REDD+. As the MRV mechanism is looking for a tool that is operational, inexpensive, practical, and which can be applied frequently for monitoring over extensive area.

5.5. TLS point cloud data

TLS acquires three-dimensional data on standing trees rapidly and accurately. The plot level data is processed to derive tree level stand parameters (Dassot et al., 2011). The use of TLS for forest inventory is relatively new and the methods for extracting structural attributes are still being refined (Lovell et al., 2011). The data processing technology has improved significantly with encouraging results (Dassot et al., 2011). The processing results of this particular study in Royal Belum will be discussed in the following sections.

5.5.1 Multiple scanning and registration

Findings of this study indicated that the registration demonstrated an average 1.03 cm of standard deviation. Registration of the multiple scans was carried out by software that uses corresponding tie points. The low standard deviation of the registration indicates that the orientation of three outer scans in

120^0 and increased number of tie points (16 in number) has played an important role in overlapping the area between the multiple scans to cover the trees parts from different directions. This is supported by Thies et al. (2004), who mention the importance of selection in orientation and overlapping area between the multiple scan positions. Additionally, Bienert & Maas (2009) pointed out the selection of a clear view of scan positions for multiple scan positions and the objective of tie points for automatic and manual registration (Figure 35). Results of the study made by Simonse et al. (2003) reported approximate error of 5 cm for tree location. While Thies et al. (2004) applied multiple scans but did not indicate the results.

For registration of multiple scans a minimum of 3 tie points is required (Bienert et al., 2007). In the study the use of many tie points enhanced the number of minimum tie points required for registration because of complex stand growth and high under growth. It should be noted, however, that increasing the number of tie points increases the time for tie points scanning, thereby increasing the time of scanning. However, it is advisable to increase the number of tie points (more than 3) depending on the degree of complexity of stand growth and under growth of the study area.

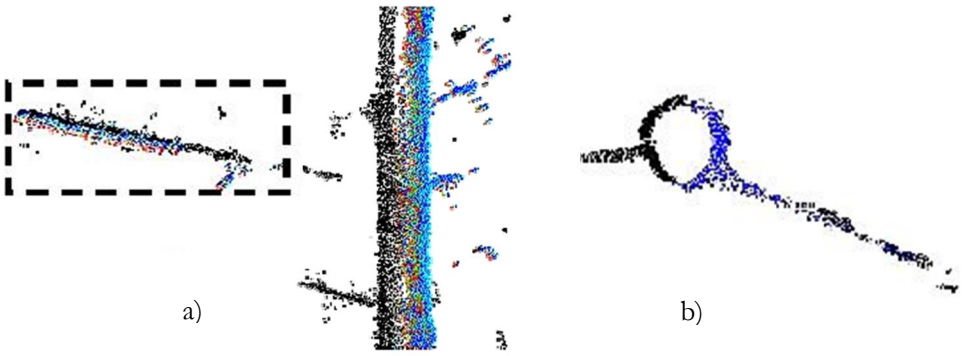

Figure 35. Illustration of a registered tree profile (Bienert & Maas, 2009) – a) detailed view of a stem of a tree and branch of a tree b) manual registration

5.5.2 Filtering and tree extration

Filtering with the range of 25 meters was performed prior to tree extraction to exclude trees outside the plot. This range of 25 meters was necessary because a filtering range of 12.62 m resulted in excluding long tree apexes. Aschoff et al. (2004) and Simonse et al. (2003) reported the importance and range (60m) of filtering of point cloud data and Bienert et al. (2006) used 12 m filtering range to remove noise and clip the data to exclude trees outside the plot. In addition, they have mentioned also the two most important things, the position and dimension in extracting trees. Furthermore, Bienert et al. (2007) used horizontal cut to segment the point cloud data to automatically detect trees. Whereas, Pfeifer et al. (2004) used manual segmentation of point cloud data. In this study tree were identified using numbered posts and segmentation was done manually. Finding of the study disclosed that with the multiple scan (4 scans) out of 698 trees, 604 trees were able to be extracted. This indicates the tree detection rate of 87 %. Bienert et al. (2007) noted automatic detection of 97.4% using single scan for primary forest (between 65-140 years) with mixed coniferous and deciduous trees with less undergrowth. Likewise, Thies et al. (2004) applied automatic tree detection to discover 26 trees out of 50 trees (52%) based on five registered scans, whereas on the basis of just one scan 11 trees (22%) were found. The finding indicates that increasing the number of multiple scans enhances tree detection. However complexity of the forest depends upon the degree of density in stand growth, slope and extent of undergrowth. These are the reasons that can be mentioned for high tree occlusion.

5.5.3 Extraction of tree DBH and height

Determination of tree height for 604 trees was carried out as the difference between the lowest point (Z-value) and the highest point from the polydata of the individual trees. Hopkinson et al. (2004) applied the approach of using the difference between the lowest point (Z-value) and the highest point inside the cut of cylinder to determine height. Similarly, Antonarakis (2011) measured height as the difference between the apex of the tree canopy and tree lowest point of the visible trunk. DBH of 604 trees was determined

by measuring all points situated in a layer 1.30 meters above the ground to the tree trunks and marking the points to separate from the other point clouds. DBH was measured manually using a measuring function which is integrated in the analysis software. Similarly, Thies et al. (2004) study first applied durably marked DBH (1.30) of each single tree in the forest with reflecting tape to take manual measurements in forest inventory. Later, he determined DBH using manual measurement analysis software.

Simonse et al. (2003) compared TLS derived tree parameters with field inventories and the results showed errors of approximately 1.7 cm for DBH. Hopkinson et al. (2004) also revealed 1.5 m error for height measurements in coniferous and deciduous forests.

Figure 36. Intensity image of a part of the sample plot. Reflecting tapes marks a height of 1.30 above ground (Thies et al., 2004)

Similarly, studies made by Sium (2015) in tropical rain forest of Royal Belum in Malaysia showed errors of 2.9 cm (14.5%) in DBH and 3.3 m (20.7%) for height. The result indicated that TLS measured tree parameters have variations to those obtained by the field inventory.

In addition to the acceptable accuracy, the frequent scan records of these measurements allows an approach to be developed for forest inventory for temporal monitoring of forest (Watt & Donoghue, 2005). This provides the tool and the method to support the monitoring, reporting and verification (MRV) for REDD projects.

5.6. Relationship of FCD with TLS parameters and Biomass

Canopy is the horizontal stretch ceiling of a forest that shows the amount and spatial distribution of above ground biomass. According to Drake et al. (2003) canopy extends from top to bottom in a three dimensional arrangement of canopy elements (leaves, branch and trunk of a tree), which means that there is also vertical extension to the horizontal one. He further discussed the dynamic nature of forest canopy structure both in time and space. The changes occur in horizontal (increase in basal area) and vertical (increase in stand height). Thus there exists an interconnection in vertical structure and above ground biomass as well. Measurement of the forest canopy cannot be acquired directly, and it must be derived from ground based empirical relationship (Fiala et al., 2006). Thus FCD mapper is a tool that measures the status of the canopy of the forest. The study explored the relationship between FCD, which is the horizontal dimension of the forest with the vertical dimensions derived from TLS parameters. Since FCD is a measure of area of the canopy, the best relationship was observed when it is related to the basal area (cross sectional area at breast height) of the plot, which means the sum of the basal area of the trees found inside the plot. The relationship was based on 20 plots. Plots with missing trees, which caused considerable decrease of basal area to obscure the relationship, were disregarded (see Figure 18). The result showed that there is a strong linear relationship with correlation coefficient value of 0.8 (see Figure 27). Torres & Lovett (2012) reported the deficiencies in a non-linear relationship are due to allometric equations, which tend to decrease biomass while diameter increases. This is because some allometric equations have limits on diameter. Similarly, O'Grady et al. (2000) and Slik et al. (2010) found biomass strong correlation to basal area. Furthermore, the findings of this study agree with those of several other studies which found a strong correlation between LiDAR metrics and above-ground biomass (Drake et al., 2002; Lefsky et al., 1999).

For investigating the relationship between FCD classes and biomass is concerned the same plots were used. The biomass of the plots was calculated using an allometric equation. The plot size (500 m^2) is

almost about half size of the pixel size (900 m²) of the map and then it was upscaled to cover the entire pixel of the FCD map. The findings indicated that a strong nonlinear relationship with correlation coefficient value of 0.91 (see Figure 28). The study demonstrated the relationships between FCD and tree stand as well as FCD and plot level parameters. This revealed the fact that there is a relationship among the three dimensional elements of the canopy. Then the FCD was regressed to biomass for upscaling the estimation of biomass/carbon of the study area. The summary of the relationships between FCD and TLS parameters, basal area and canopy is illustrated in Figure 37.

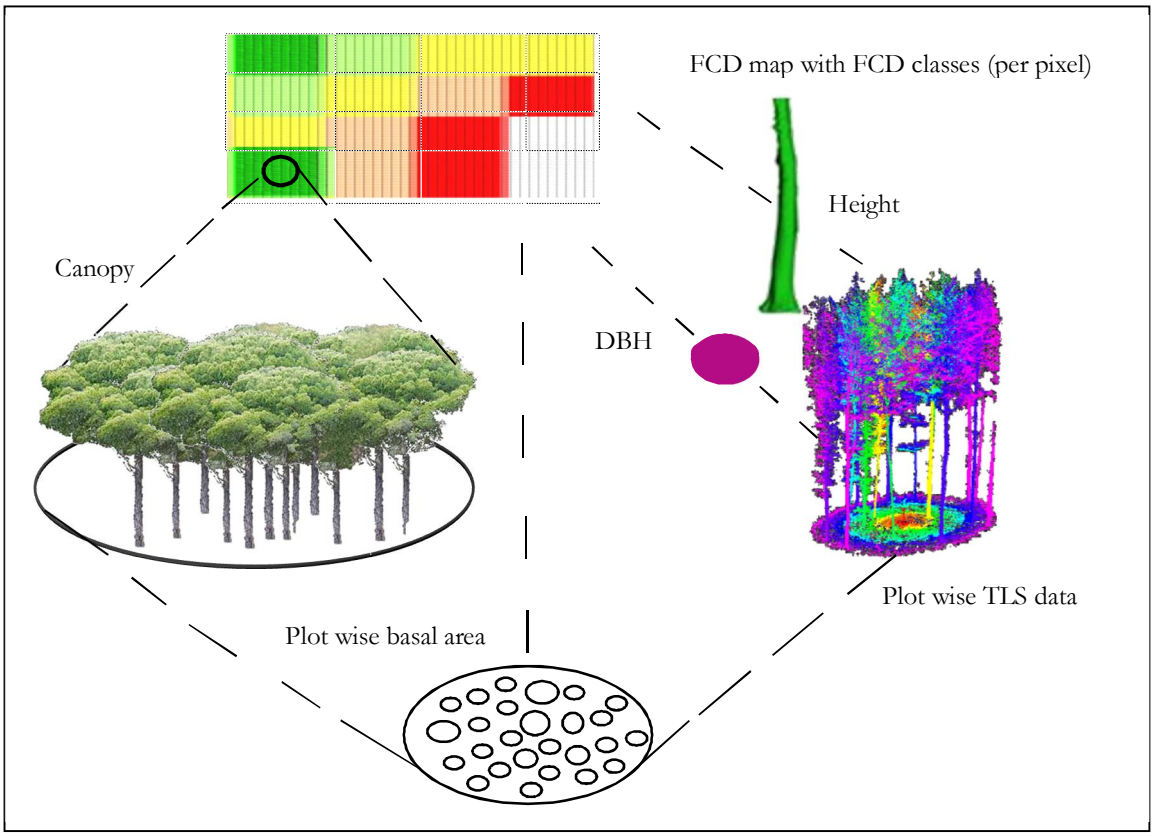

Figure 37. Relationship of FCD classes with tree stand and plot level parameters

5.7. AGB Model development and validation

For the distribution of 601 trees, the normality test of trees showed a positive skew for tree attributes of diameter (DBH) and height (H) which is non-normal (Appendix 5). Before applying allometric equation to calculate plot wise AGB these variables need to be transformed to improve hetroscedasticity. There is no standard procedure for transformation (Chave et al., 2005), but several studies suggest logarithmic transformed results in homoscedasticity (Zianis & Mencuccini, 2004). For this reason, the variables in this study were log transformed.

A nonlinear relationship was established between FCD and biomass and a Quadratic regression model was developed using 13 plots. The coefficient of determination (R^2) of the model is 66% which means 66% of variables can be explained by the model. The summary of fit of the model developed is presented (see figure 29). Chave et al. (2005) stated that the goodness of fit measures the deviation between the predicted and measured. The goodness of fit is important based on the empirical relationship chosen (Ketterings et al., 2001).

The model was then validated using 7 plots. The coefficient of determination (R^2) of the model is 73% which means that 73% of variables can be explained by the model. The summary of fit of the model developed is presented (see figure 30). Models with higher adjusted R^2 and low RMSE are indicative of better predictive ability of biomass estimation from LiDAR-derived variables (Zhao et al., 2012).

The model used general allometric equation from IPCC (IPCC, 2006). Chave et al. (2005) mentioned grouping species by broad forests types is more effective than generating species-specific allometric equations. Moreover, generic allometric equations must be employed since local equations will not improve accuracy significantly (Chave et al., 2005).

5.8. Carbon mapping

Finding of the study indicated the estimation of the total above ground biomass in the study area was 344 $MgHa^{-1}$ with RMSE value of 4.3, which is approximately 31%. According to IPCC guidelines the range of above ground biomass of tropical rain forest in Asia is between 120-680 $MgHa^{-1}$ (IPCC, 2006). Similarly, Boscolo et al. (2001) study made in Malaysia found that the average above ground biomass of 428 tons/ha. The finding of these studies is closer to the results of this study.

As a summary of the findings of this research work, it can be concluded that using Landsat-8 ETM+ images and TLS we can assess AGB/carbon to approximately 84% accurate. Knowing that Landsat images are free, one country depending on the size of forest area can use few to several TLSs to come up with reasonable estimate of carbon in a very short time and inexpensive cost.

6. CONCLUSIONS AND RECOMMENDATIONS

The method applied in this research uses Terrestrial Laser Scanner (TLS) and Landsat-8 ETM+ data for upscaling the estimation of tropical rain forest above ground biomass/carbon stock. The method is operational, inexpensive, practical, rapid and accurate, which suggests that it can be applied frequently for monitoring extensive areas in order to meet REDD+ requirements for Monitoring Reporting and Verification (MRV). In relation to the main objective and each research question, the following conclusions were drawn.

6.1. Conclusions

How is the application of classification of FCD mapper work with Landsat-8 ETM+?
FCD mapper classification found to be rapid, robust, not labour intensive and technically easy to use.

What is the accuracy of FCD classification?
The overall accuracy of the FCD classification resulted to 0.84 or 84% correlation coefficient value.

What is the relationship between FCD classes and biomass/carbon from TLS measurements?
The correlation analysis indicated a strong relationship with correlation coefficient value of 0.91 between FCD classes and biomass/carbon from TLS measurements.

How can a predictive model for up scaling biomass/carbon estimation using the above relationship be formulated?
A strong relationship between FCD classes and biomass/carbon from TLS measurements was first established and a quadratic regression model was developed. The developed model had a prediction accuracy of 66%.

What is the accuracy of the model for biomass/carbon estimation from TLS measurements?
The accuracy of the model for biomass/carbon estimation from TLS measurements was 73%.

How much carbon is stored in the study area?
The total amount of carbon stock in the study area was 556,810Mg and 162MgHa^{-1} carbon.

6.2. Recommendations

- This work need to be repeated in another tropical forest to see if the results will be similar or not.
- Manual processing is time consuming and labour intensive in consideration of the feasibility of terrestrial scanner use for efficient analysis.
- Increasing the number of multiple scans enhance the rate (percentage) of tree detection.
- More tree parameters such as stem density, stem volume, basal area etc. can be used for forest above ground biomass estimation.
- The effect of slope in TLS point cloud data need to be studied.
- It is advisable to mark DBH at 1.30 m using reflective tape during scanning to identify the exact spot where measurement can be done to minimize error encountered during measurement.

LIST OF REFERENCES

Achard, F., Eva, H. D., Mayaux, P., Stibig, H.-J., & Belward, A. (2004). Improved estimates of net carbon emissions from land cover change in the tropics for the 1990s. *Global Biogeochemical Cycles*, *18*(2).

Aikawa, S., Takao, G., Tanaka, S., Toma, T., Ehara, M., Hirata, Y., … Suzuki, K. (2012). *Cook Book, How to measure and monitor forest carbon* (No. ISBN 978-4-905304-15-9) (p. 160). Retrieved from http://www.ffpri.affrc.go.jp/redd-rdc/en/reference/cookbook/redd_cookbook_all_low_en_20121217.pdf#page=138

Antonarakis, A. S. (2011). Evaluating forest biometrics obtained from ground lidar in complex riparian forests. *Remote Sensing Letters*, *2*(1), 61–70. doi:10.1080/01431161.2010.493899

Aschoff, T., Thies, M., & Spiecker, H. (2004). Describing forest stands using terrestrial laser-scanning raw data creation the pre-filter of raw data automatic recognition of trees tin tree. *International Archives of Photogrammetry, Remote Sensing and Spatial Information Sciences*, *2*, 5.

Asner, G. P. (2001). Cloud cover in Landsat observations of the Brazilian Amazon. *International Journal of Remote Sensing*, *22*(18), 3855–3862. doi:10.1080/01431160010006926

Azizi, Z., Najafi, A., & Sohrabi, H. (2008). Forest canopy density estimating, using satellite images. In *ISPRS Congres Beijing 2008* (p. 4). Beijing.

Baccini, A., Friedl, M. A., Woodcock, C. E., & Warbington, R. (2004). Forest biomass estimation over regional scales using multisource data. *Geophysical Research Letters*, *31*(10), L10501. doi:10.1029/2004GL019782

Baynes, J. (2004). Assessing forest canopy density in a highly variable landscape using Landsat data and FCD Mapper software. *Freepatentsonline*. Retrieved from http://www.freepatentsonline.com/article/Australian-Forestry/196730172.html

Bienert, A., & Maas, H. (2009). Methods for the automatic geometric registration of terrestraial laser scanner point clouds in forest stands. *International Archives of Photogrammetry and Remote Sensing*, *32*(3/W8), 93–98.

Bienert, A., Scheller, S., Keane, E., Mohan, F., & Nugent, C. (2007). Tree detection and diameter estimations by analysis of forest terrestrial laserscanner point clouds. *International Archives of Photogrammetry and Remote Sensing*, *36*(3), 50–55.

Bienert, A., Scheller, S., Keane, E., Mullooly, G., & Mohan, F. (2006). Application of Terrestrial Laser Scanners for the determination of forest inventory parameters. *International Archives of Photogrammetry, Remote Sensing and Spatial Information Sciences*, *36*, 5.

Boscolo, M., Buongiorno, J., & Panayotou, T. (2001). Simulating options for carbon sequestration through improved management of a lowland tropical rainforest. *Environment and Development Economics*, *2*(3), 241–263.

Breidenbach, J., Næsset, E., Lien, V., Gobakken, T., & Solberg, S. (2010). Prediction of species specific forest inventory attributes using a nonparametric semi-individual tree crown approach based on fused airborne laser scanning and multispectral data. *Remote Sensing of Environment*, *114*(4), 911–924.

Brown, S. (1997). *Estimating Biomass and Biomass Change of Tropical Forests: A Primer* (No. 134) (p. 55). Rome: Food & Agriculture Org. Retrieved from http://books.google.com/books?hl=en&lr=&id=uv-ISezvitwC&pgis=1

Brown, S. (2002). Measuring carbon in forests: current status and future challenges. *Environmental Pollution*, *116*(3), 363–372. doi:10.1016/S0269-7491(01)00212-3

Cerbu, G. A., Swallow, B. M., & Thompson, D. Y. (2011). Locating REDD: A global survey and analysis of REDD readiness and demonstration activities. *Environmental Science & Policy*, *14*(2), 168–180. doi:10.1016/j.envsci.2010.09.007

Chandrashekhar, M. B., Saran, S., Raju, P. L. N., & Roy, P. S. (2005). Forest Canopy Density Stratification: How Relevant is Biophysical Spectral Response Modelling Approach? *Geocarto International*, *20*(1), 15–21. doi:10.1080/10106040508542332

Chave, J., Andalo, C., Brown, S., Cairns, M. a, Chambers, J. Q., Eamus, D., … Yamakura, T. (2005). Tree allometry and improved estimation of carbon stocks and balance in tropical forests. *Ecosystem Ecology*, *145*(1), 87–99. doi:10.1007/s00442-005-0100-x

Côté, J.-F., Widlowski, J.-L., Fournier, R. A., & Verstraete, M. M. (2009). The structural and radiative consistency of three-dimensional tree reconstructions from terrestrial lidar. *Remote Sensing of Environment*, *113*(5), 1067–1081. doi:10.1016/j.rse.2009.01.017

Dassot, M., Constant, T., & Fournier, M. (2011). The use of terrestrial LiDAR technology in forest science: application fields, benefits and challenges. *Annals of Forest Science*, *68*(5), 959–974.

DeFries, R., Achard, F., Brown, S., Herold, M., Murdiyarso, D., Schlamadinger, B., & de Souza, C. (2007). Earth observations for estimating greenhouse gas emissions from deforestation in developing countries. *Environmental Science & Policy*, *Volume 10*(4), Pages 385–394. doi:10.1016/j.envsci.2007.01.010

Deka, J., Tripathi, O. P., & Khan, M. L. (2012). Implementation of Forest Canopy Density Model to Monitor Tropical Deforestation. *Journal of the Indian Society of Remote Sensing*, *41*(2), 469–475.

Dong, J., Kaufmann, R. K., Myneni, R. B., Tucker, C. J., Kauppi, P. E., Liski, J., … Hughes, M. K. (2003). Remote sensing estimates of boreal and temperate forest woody biomass: carbon pools, sources, and sinks. *Remote Sensing of Environment*, *84*(3), 393–410. doi:10.1016/S0034-4257(02)00130-X

Drake, J. B., Dubayah, R. O., Clark, D. B., Knox, R. G., Blair, J. B., Hofton, M. a, … Prince, S. (2002). Estimation of tropical forest structural characteristics using large-footprint lidar. *Remote Sensing of Environment*, *79*(2-3), 305–319. doi:10.1016/S0034-4257(01)00281-4

Drake, J. B., Knox, R. G., Dubayah, R. O., Clark, D. B., Condit, R., Blair, J. B., & Hofton, M. (2003). Above-ground biomass estimation in closed canopy Neotropical forests using lidar remote sensing: factors affecting the generality of relationships. *Global Ecology and Biogeography*, *12*(2), 147–159. doi:10.1046/j.1466-822X.2003.00010.x

Dubayah, R. O., & Drake, J. B. (2000). Lidar Remote Sensing for Forestry. *Journal of Forestry*, *6*(98), 44–46. Retrieved from http://www.ingentaconnect.com/content/saf/jof/2000/00000098/00000006/art00015

FAO. (2004). National forest inventory: Field manual template. *The Forest Resources Assessment Programme*. Retrieved December 15, 2014, from http://www.un-redd.org/Stakeholder_Engagement/Guidelines_On_Stakeholder_Engagement/tabid/55619/Default.aspx

FAO. (2012). *FAO, State of the World's Forests 2012*, 6. Retrieved from http://www.fao.org/docrep/016/i3010e/i3010e00.htm

Fiala, A. C. S., Garman, S. L., & Gray, A. N. (2006). Comparison of five canopy cover estimation techniques in the western Oregon Cascades. *Forest Ecology and Management*, *232*(1-3), 188–197. doi:10.1016/j.foreco.2006.05.069

Fowler, A., & Kadatskiy, V. (2010). Multiple sensor platforms, *ISPRS Technical Commission IV & AutoCarto in conjunction with ASPRS/CaGIS 2010 Fall Specialty Conference. International Society of Photogrammetry and Remote Sensing* (Vol. 4, p. 4).

Gelens M.F., Van Leeuwen L.M., & Hussin Y.A. (2010). *Geo-information applications for off-reserve tree management* (p. 31).

Gibbs, H. K., Brown, S., Niles, J. O., & Foley, J. A. (2007). Monitoring and estimating tropical forest carbon stocks: making REDD a reality. *Environmental Research Letters*, *2*. doi:10.1088/1748-9326/2/4/045023

Harrell, P. A., Bourgeau-Chavez, L. L., Kasischke, E. S., French, N. H. F., & Christensen, N. L. (1995). Sensitivity of ERS-1 and JERS-1 radar data to biomass and stand structure in Alaskan boreal forest. *Remote Sensing of Environment*, *54*(3), 247–260. doi:10.1016/0034-4257(95)00127-1

Harrell, P. A., Kasischke, E. S., Bourgeau-Chavez, L. L., Haney, E. M., & Christensen, N. L. (1997). Evaluation of approaches to estimating aboveground biomass in Southern pine forests using SIR-C data. *Remote Sensing of Environment*, *59*(2), 223–233. doi:10.1016/S0034-4257(96)00155-1

Henry, M., Picard, N., Trotta, C., & Manlay, R. (2011). Estimating tree biomass of sub-Saharan African forests: a review of available allometric equations. *Silva Fennica*, *45*(3B), 477–569.

Heritage, G. L., & Large, A. R. G. (2009). *Laser Scanning for the Environmental Sciences* (First., p. 288). West sussex: Wiley-blackwell. Retrieved from http://books.google.com/books?hl=en&lr=&id=pm6DbUGNR7gC&pgis=1

Holmgren, J., Nilsson, M., & Olsson, H. (2003). Estimation of Tree Height and Stem Volume on Plots Using Airborne Laser Scanning. *Forest Science*, *49*(10), 419–428. Retrieved from http://www.ingentaconnect.com/content/saf/fs/2003/00000049/00000003/art00009

Hopkinson, C., Chasmer, L., Young-Pow, C., & Treitz, P. (2004). Assessing forest metrics with a ground-based scanning lidar. *Canadian Journal of Forest Research*, *34*(3), 573–583. doi:10.1139/x03-225

Houghton, R. A., Lawrence, K. T., Hackler, J. L., & Brown, S. (2001). The spatial distribution of forest biomass in the Brazilian Amazon: a comparison of estimates. *Global Change Biology*, *7*(7), 731–746.

Hougton, R. A. (1996). *Forest Ecosystems, Forest Management and the Global Carbon Cycle.* (M. J. Apps & D. T. Price, Eds.) (pp. 117–134). Berlin, Heidelberg: Springer Berlin Heidelberg. doi:10.1007/978-3-642-61111-7

Husch, B., Beers, T. W., Kershaw, J. A., & Jr. (2002). *Forest Mensuration* (p. 456). John Wiley & Sons. Retrieved from http://books.google.com/books?hl=en&lr=&id=p0v3m8Pau-kC&pgis=1

Hussin, Y. A. (2000). *Dissemenation of new remote sensing methodology through a semi-expert system* (Vol. 1, pp. 1–43). Enschede, Netherlands.

IPCC. (2006a). *Good practice quidlines for National Greenhouse gas inventories, Switherland: Intergovernmental panel on climate change. IPCC* (p. 83).

IPCC. (2006b). *Volume 4: Agriculture, forestry and other land use (AFOLU)* (Vol. 4, p. 673).

IPCC. (2007). *Climate Change 2007: The physical science basis. Climate Change. [Synthesis Report]* (p. 52).

ITC. (2012). The core of GIScience: a system-based approach. (V. Tolpekin & A. Stein, Eds.) (p. 524). Enschede, Netherlands: The International Institute for Geo-information and Earth Observation (ITC).

Jamalabad, M. ., & Abkar, A. A. (2004). Forest canopy density monitoring, using satellite images. In *XXth ISPRS Congress* (pp. 12–23). Istanbul.

Joshi, C., Leeuw, J. De, Skidmore, A. K., Duren, I. C. van, & van Oosten, H. (2006). Remotely sensed estimation of forest canopy density: A comparison of the performance of four methods. *International Journal of Applied Earth Observation and Geoinformation*, *8*(2), 84–95. doi:10.1016/j.jag.2005.08.004

Kandel, D. L. ., Hussin, Y. A. ., & Gelens, M. (2004). Assessing the effects of different forest management regimes on forest condition in Chitwan, Nepal, using satellite remotely sensed data and forest canopy density mapper. In *ACRS* (pp. 686–691). Chiang Mai, Thailand.

Kangas, A., & Maltamo, M. (2006). *Forest Inventory: Methodology and Applications* (p. 382). Dordrecht, Netherlands: Springer Science & Business Media. Retrieved from http://books.google.com/books?hl=en&lr=&id=zF7DOgm6MbEC&pgis=1

Kankare, V., Holopainen, M., Vastaranta, M., Puttonen, E., Yu, X., Hyyppä, J., … Alho, P. (2013). Individual tree biomass estimation using terrestrial laser scanning. *ISPRS Journal of Photogrammetry and Remote Sensing*, *75*, 64–75. doi:10.1016/j.isprsjprs.2012.10.003

Kasischke, E. S., Melack, J. M., & Craig Dobson, M. (1997). The use of imaging radars for ecological applications—A review. *Remote Sensing of Environment*, *59*(2), 141–156. doi:10.1016/S0034-4257(96)00148-4

Katoh, M., Gougeon, F. a., & Leckie, D. G. (2008). Application of high-resolution airborne data using individual tree crowns in Japanese conifer plantations. *Journal of Forest Research*, *14*(1), 10–19. doi:10.1007/s10310-008-0102-8

Ketterings, Q. M., Coe, R., van Noordwijk, M., Ambagau', Y., & Palm, C. a. (2001). Reducing uncertainty in the use of allometric biomass equations for predicting above-ground tree biomass in mixed secondary forests. *Forest Ecology and Management*, *146*(1-3), 199–209. doi:10.1016/S0378-1127(00)00460-6

King, D. a., Davies, S. J., Supardi, M. N. N., & Tan, S. (2005). Tree growth is related to light interception and wood density in two mixed dipterocarp forests of Malaysia. *Functional Ecology*, *19*(3), 445–453. doi:10.1111/j.1365-2435.2005.00982.x

Kwon, T., Lee, W., Kwak, D., Park, T., Lee, J. Y., Hong, S. Y., … Kim, S. R. (2012). Forest Canopy Density Estimation Using Airborne Hyperspectral Data. *Korean Journal of Remote Sensing*, *28*(3), 297–305.

Lefsky, M. A., Cohen, W. B., Acker, S. A., Parker, G. G., Spies, T. A., & Harding, D. (1999). Lidar Remote Sensing of the Canopy Structure and Biophysical Properties of Douglas-Fir Western Hemlock Forests. *Remote Sensing of Environment*, *70*(3), 339–361. doi:10.1016/S0034-4257(99)00052-8

Lefsky, M. A., Cohen, W. B., Parker, G. G., & Harding, D. J. (2002). Lidar Remote Sensing for Ecosystem Studies. *BioScience*, *52*(1), 19.

Lefsky, M. A., Harding, D., Cohen, W. ., Parker, G., & Shugart, H. . (1999). Surface Lidar Remote Sensing of Basal Area and Biomass in Deciduous Forests of Eastern Maryland, USA. *Remote Sensing of Environment*, *67*(1), 83–98. doi:10.1016/S0034-4257(98)00071-6

Lillesand, T. M., Kiefer, R. W., & Chipman, J. W. (2004). *Remote sensing and image interpretation.* (4th ed.). Chichester, UK: John Wiley & Sons Ltd. Retrieved from http://www.cabdirect.org/abstracts/20043080717.html;jsessionid=D128E974F44E6F3E84E77401581AA674

Lopez Bautista, A. A. (2012). *Biomass/carbon estimation and mapping in the subtropical forest of Chitwan , Nepal: A comparison between VHR GeoEye satellite images and airborne LiDAR data*. http://www.itc.nl/library/AcadamicOutputs/MSc thesis/2012/NRM/lopezbautista.pdf.

Lovell, J. L., Jupp, D. L. B., Newnham, G. J., & Culvenor, D. S. (2011). Measuring tree stem diameters using intensity profiles from ground-based scanning lidar from a fixed viewpoint. *ISPRS Journal of Photogrammetry and Remote Sensing*, *66*(1), 46–55. doi:10.1016/j.isprsjprs.2010.08.006

Lu, D. (2006). The potential and challenge of remote sensing-based biomass estimation. *International Journal of Remote Sensing*, *27*(7), 1297–1328. doi:10.1080/01431160500486732

Lu, D. (2007). Aboveground biomass estimation using Landsat TM data in the Brazilian Amazon. *International Journal of Remote Sensing*, *26*(12), 2509–2525. doi:10.1080/01431160500142145

Lu, D., Chen, Q., Wang, G., Moran, E., Batistella, M., Zhang, M., … Saah, D. (2012). Aboveground Forest Biomass Estimation with Landsat and LiDAR Data and Uncertainty Analysis of the Estimates. *International Journal of Forestry Research*, *2012*(1), 1–16.

Luckman, A., Baker, J., Kuplich, T. M., Freitas, C., & Frery, A. C. (1997). A Study of the Relationship between Radar Baekseatter and Regenerating Tropical Forest Biomass for Spaeeborne SAR Instruments i i. *Remote Sensing of Environment*, *60*(1-13).

Maan, G. S., Singh, C. K., Singh, M. K., & Nagarajan, B. (2014). Tree species biomass and carbon stock measurement using ground based-LiDAR. *Geocarto International*, (July), 1–18.

Maas, H. -G., Bienert, A., Scheller, S., & Keane, E. (2008). Automatic forest inventory parameter determination from terrestrial laser scanner data. *International Journal of Remote Sensing*, *29*(5), 1579–1593.

Magnussen, S., Eggermont, P., & LaRiccia, V. N. (1999). Recovering Tree Heights from Airborne Laser Scanner Data. *Forest Science*, *45*(3), 407–422. Retrieved from http://www.ingentaconnect.com/content/saf/fs/1999/00000045/00000003/art00012

Maharjan, S. (2012). Estimation and mapping above ground woody carbon stocks using Lidar data and digital camera imagery in the hilly forests of Gorkha, NEPAL. http://www.itc.nl/library/AcadamicOutputs/MSc thesis/2012/NRM/maharjan.pdf.

Mon, S. M., Mizoue, N., Htun, N. Z., Kajisa, T., & Yoshida, S. (2012). Estimating forest canopy density of tropical mixed deciduous vegetation using Landsat data: a comparison of three classification approaches. *International Journal of Remote Sensing*, *33*(4), 1042–1057.

Musa, S., Kassim, A. R., Yusoff, S. M., & Ibrahim, S. (2003). Assessing the status of logged-over production forests: The development of a rapis appraisal technique. *FAO*. Retrieved December 26, 2014, from http://www.fao.org/docrep/008/ae578e/ae578e00.htm

Nandy, S., Joshi, P. K., & Das, K. K. (2003). Forest canopy density stratification using biophysical modeling. *Journal of the Indian Society of Remote Sensing*, *31*(4), 291–297. doi:10.1007/BF03007349

Nelson, R. F., Kimes, D. S., Salas, W. a., & Routhier, M. (2000). Secondary Forest Age and Tropical Forest Biomass Estimation Using Thematic Mapper Imagery. *BioScience*, *50*(5), 419.

Noble, I., & Scholes, R. J. (2001). Sinks and the Kyoto Protocol. *Climate Policy*, *volume 1*(1), Pages 5–25. doi:10.1016/S1469-3062(00)00002-4

O'Grady, A. P., Chen, X., Eamus, D., & Hutley, L. B. (2000). Composition, leaf area index and standing biomass of eucalypt open forests near Darwin in the Northern Territory, Australia. *Australian Journal of Botany*, *48*(5), 629. doi:10.1071/BT99022

Oliveira, A. A. De, & Mori, S. A. (1999). A central Amazonian terra firme forest. I. High tree species richness on poor soils. *Biodiversity & Conservation*, *8*(9), 1219–1244. doi:10.1023/A:1008908615271

Panta, M., & Kim, K. (2006). Spatio-temporal Dynamic Alteration of Forest Canopy Density based on Site Associated Factors؛ View from Tropical Forest of Nepal. *Korean Journal of Remote Sensing*, *22*(5), 1–11.

Patenaude, G., Hill, R. ., Milne, R., Gaveau, D. L. a., Briggs, B. B. J., & Dawson, T. P. (2004). Quantifying forest above ground carbon content using LiDAR remote sensing. *Remote Sensing of Environment*, *93*(3), 368–380.

Patenaude, G., Milne, R., & Dawson, T. P. (2005). Synthesis of remote sensing approaches for forest carbon estimation: reporting to the Kyoto Protocol. *Environmental Science & Policy*, *8*(2), 161–178.

Pax-Lenney, M., Woodcock, C. E., Macomber, S. A., Gopal, S., & Song, C. (2001). Forest mapping with a generalized classifier and Landsat TM data. *Remote Sensing of Environment*, *77*(3), 241–250.

Petrokofsky, G., Kanamaru, H., Achard, F., Goetz, S. J., Joosten, H., Holmgren, P., … Wattenbach, M. (2012). Comparison of methods for measuring and assessing carbon stocks and carbon stock changes in terrestrial carbon pools. How do the accuracy and precision of current methods compare? A systematic review protocol. *Environmental Evidence*, *Volume 1*(1), page 6.

Pfeifer, N., Gorte, B., Winterhalder, D., Sensing, R., & Range, C. (2004). Automatic reconstruction of single trees from terrestrial laser scanner data. *International Society of Photogrammetry and Remote Sensing*. Retrieved from http://218.196.194.5/portal/wenxian/gis article/533.pdf

Phillips, O. L., Malhi, Y., Vinceti, B., Baker, T., Lewis, S. L., Higuchi, N., … Grace, J. (2002). Changes in growth of tropical forests: evaluating potential potential biases. *Ecological Applications*, *12*(2), 576–587.

Phua, M.-H., & Saito, H. (2003). Estimation of biomass of a mountainous tropical forest using Landsat TM data. *Canadian Journal of Remote Sensing*, *29*(4), 429–440. doi:10.5589/m03-005

Popescu, S. C. (2007). Estimating biomass of individual pine trees using airborne lidar. *Biomass and Bioenergy*, *31*(9), 646–655. doi:10.1016/j.biombioe.2007.06.022

Popescu, S. C., Wynne, R. H., & Nelson, R. F. (2003). Measuring individual tree crown diameter with lidar and assessing its influence on estimating forest volume and biomass. *Canadian Journal of Remote Sensing*, *29*(5), 564–577.

Qureshi, A., Pariva, R. B., & Hussain, S. A. (2012). A review of protocols used for assessment of carbon stock in forested landscapes. *Environmental Science & Policy*, *Volume 16*, Pages 81–89.

Rana, B., & Vickers, B. (2005). Return of the Churia Forests. *GOPA-AGEG*, 17.

Ravindranath, N. H., & Ostwald, M. (2008). *Carbon Inventory Methods Handbook for Greenhouse Gas Inventory, Carbon Mitigation and Roundwood Production Projects* (pp. 181–199). Dordrecht: Springer Science + Business media B.V. doi:10.1007/978-1-4020-6547-7

Reimann, C., Filzmoser, P., Garrett, R., & Dutter, R. (2011). *Statistical Data Analysis Explained: Applied Environmental Statistics with R* (p. 362). John Wiley & Sons. Retrieved from https://books.google.com/books?hl=en&lr=&id=EyjYMb-mTfAC&pgis=1

Rikimaru, A., & Miyatake, S. (1997). Development of Forest Canopy Density Mapping and Monitoring Model using Indices of Vegetation , Bare soil and Shadow. *Geospatial World*. Retrieved August 25, 2014, from www.gisdevelopment.net

Rikimaru, A., Miyatake, S., & Dugan, P. (1999). Sky is the limit for forest management tool. *Tropical Forest Update*, pp. 6–8.

Rikimaru, A., Roy, P. S., & Miyatake, S. (2002). Tropical forest cover density mapping. *Tropical Ecology*, *43*(1), 39–47. Retrieved from http://www.tropecol.com/pdf/open/PDF_43_1/43104.pdf

Rosenqvista, Å., Milneb, A., Lucasc, R., Imhoffd, M., & Dobsone, C. (2003). A review of remote sensing technology in support of the Kyoto Protocol. *Environmental Science & Policy*, *volume 6*, Pages 441–455.

Roy, D. P., Borak, J. S., Devadiga, S., Wolfe, R. E., Zheng, M., & Descloitres, J. (2002). The MODIS Land product quality assessment approach. *Remote Sensing of Environment*, *83*(1-2), 62–76.

Roy, P. S., Miyatake, S., & Rikimaru, A. (1997). Biophysical spectral response modeling approach for forest density stratification. In *The 18th Asian Conference on Remote Sensing*. Kuala Lumpur, Malaysia. Retrieved from http://geospatialworld.net/Paper/Application/ArticleView.aspx?aid=505

Royal Belum State Park. (2003). Royal Belum State Park. Retrieved from http://malaysiahere.com/malaysia_wildlife/royal_belum_wildlife.php

Seidel, D., Albert, K., Ammer, C., Fehrmann, L., & Kleinn, C. (2013). Using terrestrial laser scanning to support biomass estimation in densely stocked young tree plantations. *International Journal of Remote Sensing*, *34*(24), 8699–8709. doi:10.1080/01431161.2013.848308

Simonse, M., Aschoff, T., Spiecker, H., & Thies, M. (2003). Automatic determination of forest inventory parameters (pp. 1–7). Freiburg. Retrieved from http://www.natscan.uni-freiburg.de/suite/pdf/030916_1642_1.pdf

Slik, J. W. F., Aiba, S.-I., Brearley, F. Q., Cannon, C. H., Forshed, O., Kitayama, K., … van Valkenburg, J. L. C. H. (2010). Environmental correlates of tree biomass, basal area, wood specific gravity and stem density gradients in Borneo's tropical forests. *Global Ecology and Biogeography*, *19*(1), 50–60.

Stolle, F., Parra, A., Smith, G., Angeletti, I., Banskoca, A., Kemen Austin, A., & Musisky, J. (2013). *REDD+* Measurment, Reporting and Verification (MRV) Manual. *Forest Carbon Markets and Communities* (p. 160). Arlington, USA.

Su Mon, M., Mizoue, N., Htun, N. Z., Kajisa, T., & Yoshida, S. (2012). Estimating forest canopy density of tropical mixed deciduous vegetation using Landsat data: a comparison of three classification approaches. *International Journal of Remote Sensing*, *33*(4), 1042–1057.

Sussman, R., Sweeney, S., Green, G., Porton, I., Andrianasolondraibe, O. L., & Ratsirarson, J. (2006). A preliminary estimate of Lemur catta population density using satellite imagery. *Ringtailed Lemur Biology Developments in Primatology: Progress and Prospect*, 16–31. doi:10.1007/978-0-387-34126-2

Tansey, K., Selmes, N., Anstee, a., Tate, N. J., & Denniss, a. (2009). Estimating tree and stand variables in a Corsican Pine woodland from terrestrial laser scanner data. *International Journal of Remote Sensing*, *30*(19), 5195–5209. doi:10.1080/01431160902882587

Thies, M., Pfeifer, N., Winterhalder, D., & Gorte, B. G. H. (2004). Three-dimensional reconstruction of stems for assessment of taper, sweep and lean based on laser scanning of standing trees. *Scandinavian Journal of Forest Research*, *19*(6), 571–581. doi:10.1080/02827580410019562

Thies, M., Spiecker, H., & Str, T. (2004). Evaluation and future prospects of terrestrial laser scanning for standardized laser scanning for standardized forest inventories. *International Archives of Photogrammetry and Remote Sensing*, *36*(8), 192–197.

Torres, B. A., & Lovett, J. C. (2012). Using basal area to estimate aboveground carbon stocks in forests: La Primavera Biosphere's Reserve, Mexico. *Forestry*, *86*(2), 267–281. doi:10.1093/forestry/cps084

Turner, D. P., Ritts, W. D., Cohen, W. B., Gower, S. T., Zhao, M., Running, S. W., … Munger, J. W. (2003). Scaling Gross Primary Production (GPP) over boreal and deciduous forest landscapes in support of MODIS GPP product validation. *Remote Sensing of Environment*, *88*(3), 256–270. doi:10.1016/j.rse.2003.06.005

UNFCCC. (2014). *United Nations Framework Convention on Climate Change*. Retrieved May 25, 2014, from https://unfccc.int/kyoto_protocol/items/2830.php

UN-REDD Programme. (2009). Retrieved May 25, 2014, from http://www.un-redd.org/AboutUN-REDDProgramme/tabid/102613/Default.aspx

Van der Werf, G. R., Morton, D. C., DeFries, R. S., Olivier, J. G. J., Kasibhatla, P. S., Jackson, R. B., … Randerson, J. T. (2009). CO2 emissions from forest loss. *Nature Geoscience*, *2*(11), 737–738.

Varjo, J., & Mery, G. (2001). *World Forests, Markets and Policies*. (M. Palo, J. Uusivuori, & G. Mery, Eds.) (vol 3., p. 490). Dordrecht, Netherlands: kluwer Academic Publishers. Retrieved from http://books.google.com/books?hl=en&lr=&id=PUQENz7uqdcC&pgis=1

Watt, P. J., & Donoghue, D. N. M. (2005). Measuring forest structure with terrestrial laser scanning. *International Journal of Remote Sensing*, *26*(7), 1437–1446. doi:10.1080/01431160512331337961

Wezyk, P., Koziol, K., Glista, M., & Pierzchalski, M. (2007). Terrestrial laser scanning versus traditional forest inventory first results from the Polish forests. In *ISPRS Workshop on Laser Scanning 2007 and SilviLaser 2007* (pp. 424–429). Espoo, Finland: ISPRS Workshop on Laser Scanning 2007 and SilviLaser 2007.

Wulder, M. A., Han, T., White, J. C., Sweda, T., & Tsuzuki, H. (2007). Integrating profiling LIDAR with Landsat data for regional boreal forest canopy attribute estimation and change characterization. *Remote Sensing of Environment*, *110*(1), 123–137. doi:10.1016/j.rse.2007.02.002

Yang, X., Strahler, A. H., Schaaf, C. B., Jupp, D. L. B., Yao, T., Zhao, F., … Ni-Meister, W. (2013). Three-dimensional forest reconstruction and structural parameter retrievals using a terrestrial full-waveform lidar instrument (Echidna®). *Remote Sensing of Environment*, *135*, 36–51. doi:10.1016/j.rse.2013.03.020

Yao, T., Yang, X., Zhao, F., Wang, Z., Zhang, Q., Jupp, D., … Strahler, A. (2011). Measuring forest structure and biomass in New England forest stands using Echidna ground-based lidar. *Remote Sensing of Environment*, *115*(11), 2965–2974. doi:10.1016/j.rse.2010.03.019

Zhang, X.-Q., & Xu, D. (2003). Potential carbon sequestration in China's forests. *Environmental Science and Policy*, *Volume 6*(5), Pages 421–432. doi:10.1016/S1462-9011(03)00072-8

Zhao, F., Guo, Q., & Kelly, M. (2012). Allometric equation choice impacts lidar-based forest biomass estimates: A case study from the Sierra National Forest, CA. *Agricultural and Forest Meteorology*, *165*, 64–72. doi:10.1016/j.agrformet.2012.05.019

Zheng, D., Rademacher, J., Chen, J., Crow, T., Bresee, M., Le Moine, J., & Ryu, S.-R. (2004). Estimating aboveground biomass using Landsat 7 ETM+ data across a managed landscape in northern Wisconsin, USA. *Remote Sensing of Environment*, *93*(3), 402–411. doi:10.1016/j.rse.2004.08.008

Zianis, D., & Mencuccini, M. (2004). On simplifying allometric analyses of forest biomass. *Forest Ecology and Management*, *187*(2-3), 311–332. doi:10.1016/j.foreco.2003.07.007

Appendices

Appendix 1. Tally sheet for field data recording

Field Inventory Sheet

Plot No.: Date: Time: Surveyor's:

Reference Point: Bearing: Distance:

Slope (%): Aspect: Canopy density: 1. 2. 3. 4. Average:

Center Position: X-Coordinate: Y-Coordinate: Z-coord.: FCD Class No.:

Scan Positions: 1._____ Undergrowth:

2._____

3._____

S.N.	X- Coordinate	Y- Coordinate	Z- Coordinate	DBH (cm)	Height (m)	Crown Diam (m)	Species	Remarks

Appendix 2. Slope correction table

Slope%	Radius(m)	Slope%	Radius(m)	Slope%	Radius(m)
0	12.62				
1	12.62	36	13.01	71	13.97
2	12.62	37	13.03	72	14.00
3	12.62	38	13.05	73	14.04
4	12.62	39	13.07	74	14.07
5	12.62	40	13.09	75	14.10
6	12.63	41	13.12	76	14.14
7	12.63	42	13.14	77	14.17
8	12.64	43	13.16	78	14.21
9	12.64	44	13.19	79	14.24
10	12.65	45	13.21	80	14.28
11	12.65	46	13.24	81	14.31
12	12.66	47	13.26	82	14.35
13	12.67	48	13.29	83	14.38
14	12.68	49	13.31	84	14.42
15	12.69	50	13.34	85	14.45
16	12.70	51	13.37	86	14.49
17	12.71	52	13.39	87	14.52
18	12.72	53	13.42	88	14.56
19	12.73	54	13.45	89	14.60
20	12.74	55	13.48	90	14.63
21	12.75	56	13.51	91	14.67
22	12.77	57	13.53	92	14.71
23	12.78	58	13.56	93	14.74
24	12.79	59	13.59	94	14.78
25	12.81	60	13.62	95	14.82
26	12.82	61	13.65	96	14.85
27	12.84	62	13.68	97	14.89
28	12.86	63	13.72	98	14.93
29	12.87	64	13.75	99	14.97
30	12.89	65	13.78	100	15.00
31	12.91	66	13.81	101	15.04
32	12.93	67	13.84	102	15.08
33	12.95	68	13.87	103	15.12
34	12.97	69	13.91	104	15.15
35	12.99	70	13.94	105	15.19

Source: Y.A. Hussin (2001) from lecture note

Appendix 3. Example of a Plot TLS tree parameters (DBH and height) used for data analysis

Plot No.	Tree No	TLS DBH	TLS Height	Species
1	1	22.9	11.26	*Mallothus biaceae*
1	2	16.6	17.77	*Mallothus biaceae*
1	3	27.3	18.87	*A. rigidus*
1	4	15.9	10.69	*A. rigidus*
1	5	22.1	11.35	*Mallothus biaceae*
1	6	34.2	19.61	*A. rigidus*
1	7	23.5	10.43	*Mallothus biaceae*
1	8	14.8	11.91	*Mallothus biaceae*
1	9	20.6	10.82	*syn. Acacia greggii*
1	10	15.9	10.93	*syn. Acacia greggii*
1	11	16.1	10.41	*Mastixia trichotoma Blume*
1	12	13.5	9.55	*Mastixia trichotoma Blume*

Appendix 4. Meta data of record sheet for TLS scanning

Plot No.	Slope	Scan No.	Position	X-Coordinate	Y-Coordinate	Scanning Form	Resoulution	Date	Time	Remarks

Appendix 5. Normality test

	N	Minimum	Maximum	Mean	Std. Deviation	Skewness		Kurtosis	
	Statistic	Statistic	Statistic	Statistic	Statistic	Statistic	Std. Error	Statistic	Std. Error
TLS DBH	601	10.00	111.20	22.7454	16.01043	2.556	.100	7.716	.199
TLS Height	601	4.950000000	40.25000000	15.14571215	5.856328492	1.291	.100	2.058	.199
Valid N (listwise)	601								

Appendix 6. Regression analysis for model development

SUMMARY OUTPUT

Regression Statistics	
Multiple R	0.799553
R Square	0.639285
Adjusted R Square	0.606492
Standard Error	2.824285
Observations	13

ANOVA

	df	*SS*	*MS*	*F*	*Significance F*
Regression	1	155.5033	155.5033	19.49497	0.00103654
Residual	11	87.74247	7.976588		
Total	12	243.2458			

	Coefficients	*tandard Err*	*t Stat*	*P-value*	*Lower 95%*	*Upper 95%*	*ower 95.0%*	*pper 95.0%*
Intercept	6.793102	2.777719	2.445569	0.0325	0.67938439	12.90682	0.679384	12.90682
Observe Biomass	0.628026	0.142238	4.415311	0.001037	0.31496191	0.941091	0.314962	0.941091

Appendix 7. Regression analysis for model validation

SUMMARY OUTPUT

Regression Statistics	
Multiple R	0.853128
R Square	0.727827
Adjusted R Square	0.673393
Standard Error	4.265877
Observations	7

ANOVA

	df	*SS*	*MS*	*F*	*gnificance F*
Regression	1	243.3159	243.3159	13.37069	0.014647
Residual	5	90.98855	18.19771		
Total	6	334.3044			

	Coefficients	*tandard Err*	*t Stat*	*P-value*	*Lower 95%*	*Upper 95%*	*ower 95.0%*	*Upper 95.0%*
Intercept	3.283076	3.111178	1.055252	0.339608	-4.71446	11.28061	-4.71446	11.280614
Observe Biomass	0.766987	0.209754	3.656595	0.014647	0.227796	1.306178	0.227796	1.306178

Appendix 8. Registration result of multiple scans

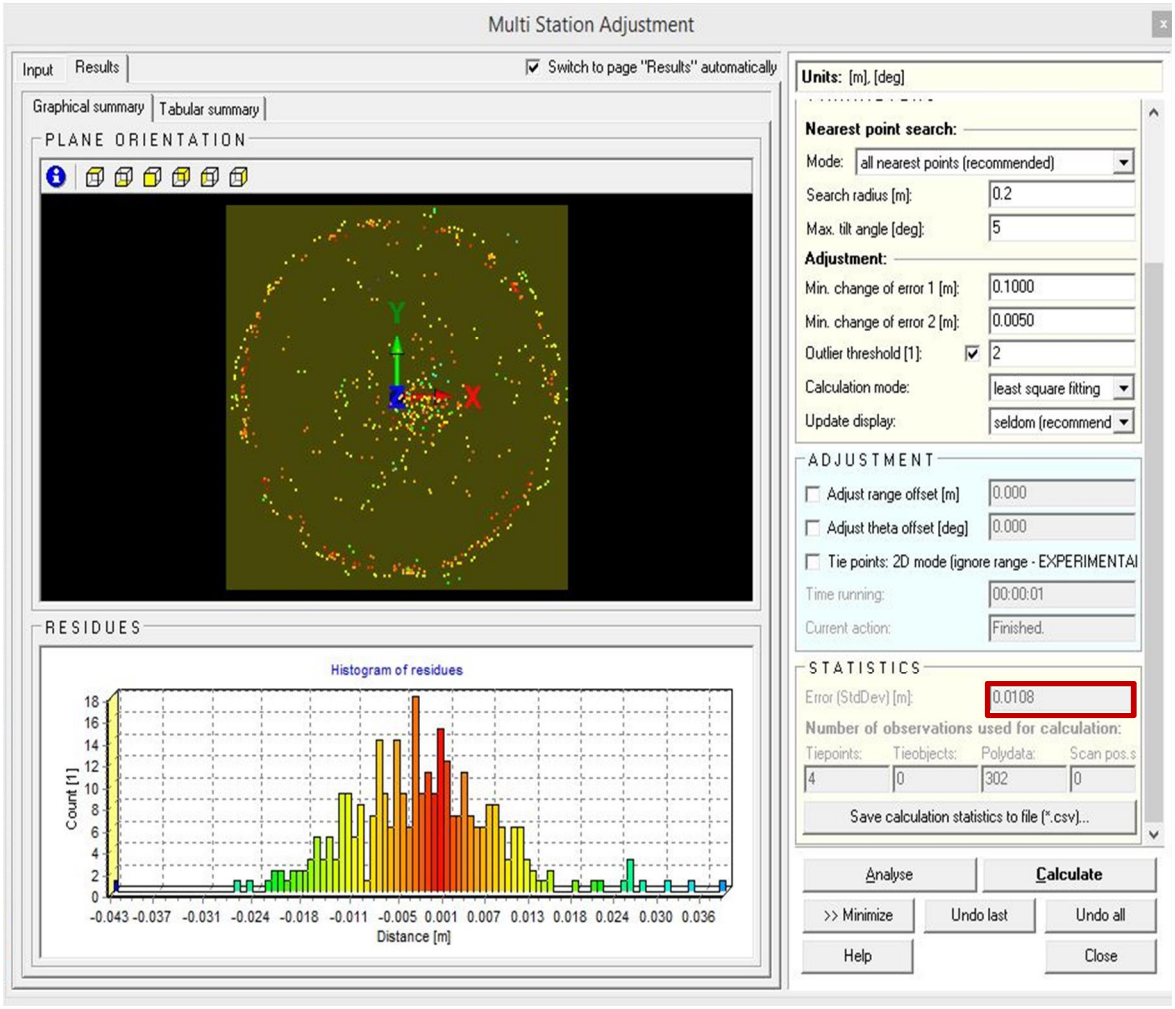

Appendix 9. CAN-EYE classification result

CALIBRATION PARAMETERS

Image Size	(2848,4272)	Optical Centre	(1412,2136)
Projection Function	3degree	Coefficient	(0.00000,-0.00001,0.05850)

SELECTED IMAGES

File	FCover (%)
IMG_0414.JPG	95.0
IMG_0423.JPG	79.9
IMG_0432.JPG	98.1
IMG_0441.JPG	90.2
IMG_0451.JPG	89.0
IMG_0460.JPG	93.5
IMG_0469.JPG	95.4
IMG_0478.JPG	99.0

NUMBER OF CLASSES : 2

Class Name	%
Sky	10.27
Green Vegetation	89.73

AVERAGE BIOPHYSICAL VARIABLES

fCover= 92.5% (std=5.8)

CLASSIFICATION RESULTS

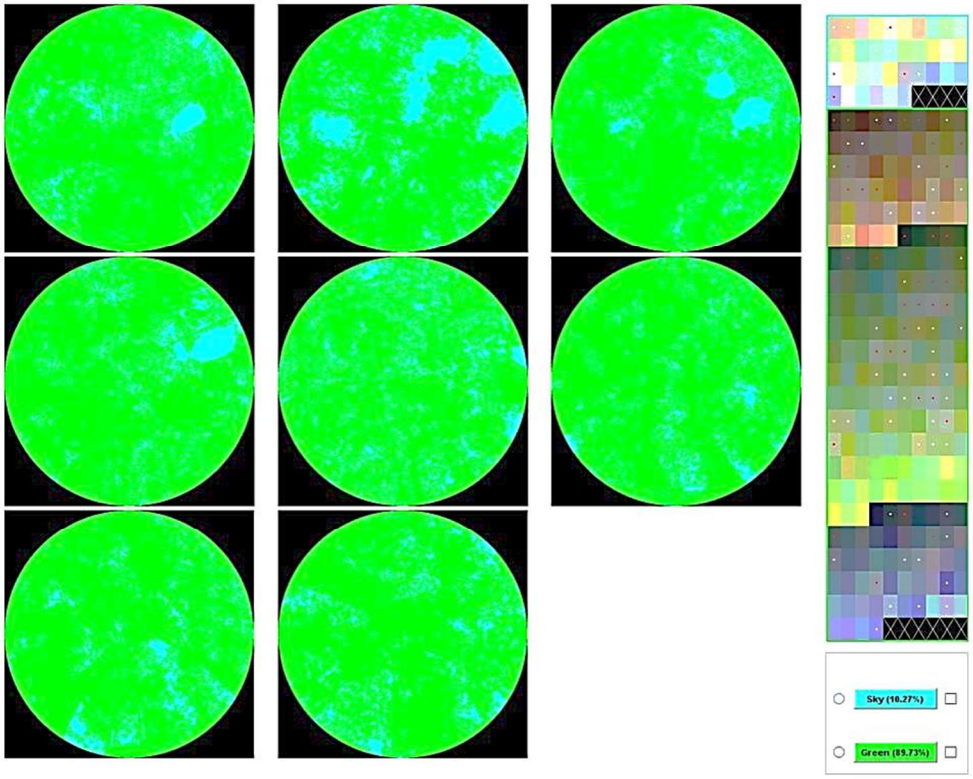

Appendix 10. Photos from the field